Impact of Grid Resolution on Atmospheric Model Simulation of Offshore Surface Wind Speed

by

Michael Bouey

A Thesis Presented in Partial Fulfillment
of the Requirements for the Degree
Master of Science

Approved May 2012 by the
Graduate Supervisory Committee:

Huei-Ping Huang, Chair
Steven Trimble
Ronald Calhoun

ARIZONA STATE UNIVERSITY

August 2012

ABSTRACT

This study considered the impact of grid resolution on wind velocity simulated by the Weather Research and Forecasting (WRF) model. The period simulated spanned November 2009 through January 2010, for which, multi-resolution nested domains were examined. Basic analysis was performed utilizing the data assimilation tools of NCEP/NCAR (National Center for Environmental Prediction/National Center for Atmospheric Research) to determine the ideal location to examine during the simulation was the Pacific Northwest portion of the United States, specifically the border between California and Oregon. The simulated mutli-resolution nested domains in this region indicated an increase in apparent wind speed as the resolution for the domain was increased. These findings were confirmed by statistical analysis which identified a positive bias for wind speed with respect to increased resolution as well as a correlation coefficient indicating the existence of a positive change in wind speed with increased resolution. An analysis of temperature change was performed in order to test the validity of the findings of the WRF simulation model. The statistical analysis performed on temperature change throughout the increased grid resolution did not indicate any change in temperature. In fact the

correlation coefficient values between the domains were found in the 0.90 range, indicating the non-sensitivity of temperature across the increased resolutions. These results validate the findings of the WRF simulation: increased wind velocity can be observed at higher grid resolution. The study then considered the difference between wind velocity observed over the entire domains and the wind velocity observed solely over offshore locations. Wind velocity was observed to be significantly higher (an increase of 68.4%) in the offshore locations. The findings of this study suggest simulation tools should be utilized to examine domains at a higher resolution in order to identify potential locations for wind farms. The results go further to suggest the ideal location for these potential wind farms will be at offshore locations.

DEDICATION

I would like to dedicate my thesis to my grandfather, Dr. Richard Perry. He was the man who first got me interested in mathematics and science. Many summer nights we would star gaze with a homemade telescope as he shared stories about research and work he did with NASA. "Who is seeing stars now, Grandpa?"

Grandpa always set the bar high, and without his example, shared passion of science, and lessons in patience, I would never have dreamt so big. This thesis is for you, Dr. Perry. I am as I was when I was a child, trying to impress the physics department head, with my science project. Thank you so much Grandpa, you mean the world to me.

ACKNOWLEDGMENTS

This thesis would never have been written if not for the help of the following:

First, and formost, I would like to thank my thesis advisor, Dr. Huei-Ping Huang. He has been the sum of all wisdom. He always had a second to spare and every time we spoke I felt as though I needed to rush to a piece of paper to write down what he said.

Second, I would like to thank Doctoral Candidate Ashish Sharma. Ashish is pursuing his Ph.D under the guidance of Dr. Huang. Ashish's experience and support during the simulation portion made the body of my research possible.

Finally, I would like to thank my Fiancée, Melissa Joy Laliberte. Through her patience, support, and love she has given me the strength to achieve my goals. She has supported me through the bulk of my education. Simply put, without Melissa, I would not have a thesis. I love you and thank you for everything.

TABLE OF CONTENTS

Page

LIST OF TABLES viii

LIST OF FIGURES ix

LIST OF SYMBOLS / NOMENCLATURE xi

CHAPTER

1 INTRODUCTION 1

1.1 Wind Energy 1

1.2 Wind Power Generation 2

1.3 The Wind Energy Industry 4

1.4 Wind Farm Site Selection 6

1.5 Weather and Surface Wind Simulation 8

1.6 Statement of Purpose 8

2 BACKGROUND LITERATURE 11

2.1 Simulation Tools and Techniques 11

2.2 Mesoscale Meteorological Modeling 12

2.3 Offshore Physics 17

3 METHODOLOGY 20

3.1 Experiment and Simulation Overview 20

3.2 Selection of Location to Examine 22

3.2.1 Initial Analysis NCEP/NCAR Reanalysis 24

3.2.2 Data Assimilation 27

CHAPTER Page

3.3 WRF Model 29
3.3.1 WRF Model Software Structure 30
3.3.2 NCEP FNL Input Data 32
3.4 Methodology Summary 33
4 DATA ANALYSIS AND RESULTS 34
4.1 WRF Model Results 34
4.2 Domain Comparison 38
4.3 Offshore Wind Magnitude Bias 39
4.4 Offshore Temperature Bias 44
5 DISCUSSION 46
5.1 Examining Extrema through Grid Resolution 46
5.2 Implications of the Existence of Bias 47
5.3 Statistical Analysis of Bias 48
5.4 Narrowing the Scope to Offshore Locations 48
5.5 Domain Correlation 50
5.6 Examining Temperature 51
6 CONCULSION 53
6.1 Summary of Findings 53
6.2 Implications of Findings 54
6.3 Suggestions for Future Research 55
6.4 Conclusion 58

Page

REFERENCES 59

APPENDIX

A ADDITIONAL FIGURES..... 64

B ADDITIONAL TABLES 74

BIOGRAPHICAL SKETCH 76

LIST OF TABLES

Table Page

1: WRF simulation setup summary 31

2: Whole domain wind speed statistics..... 42

3: Whole domain RMSE & bias statistics 43

4: Offshore domain wind speed statistics 50

5: Whole domain wind correlation 51

6: Whole domain temperature correlation 52

B-1: Offshore domain RMSE & bias..... 75

B-2: Offshore domain wind correlation..... 75

LIST OF FIGURES

Figure Page

1: Wind illustration 1

2: Mesoscale model 3D gridded domain 14

3: Sea-level breeze illustration 17

4: WRF simulated domains 20

5: Reanalysis plots – site selection 25

6: WSF framework 31

7: WRF domain 1 – wind speed plots 35

8: WRF domain 3 – wind speed plots 36

9: "Whole domain" comparison model 37

10: January 2010 side by side domain comparison 38

11: January 2010 RMSE and difference comparison 40

12: Whole domain mean wind speed statistics 41

13: RMSE & correlation coefficient wind speed statistics 43

14: Jan 2010 RMSE & difference temp comparison 45

15: "Offshore domain" comparison model 47

16: Offshore domain mean wind speed statistics 49

A-1: Domain 1, Nov 2009, wind speed 65

A-2: Domain 1, Dec 2009, wind speed 65

A-3: Domain 1, Jan 2010, wind speed 66

A-4: Domain 2, Nov 2009, wind speed 66

Figure Page

A-5: Domain 2, Dec 2009, wind speed 67

A-6: Domain 2, Jan 2010, wind speed 67

A-7: Domain 3, Nov 2009, wind speed 68

A-8: Domain 3, Dec 2009, wind speed 68

A-9: Domain 3, Jan 2010, wind speed 69

A-10: Nov 2009, wind speed comparison 69

A-11: Dec 2009, wind speed comparison 70

A-12: Jan 2010, wind speed comparison 70

A-13: Nov 2009, wind speed RMSE & bias 71

A-14: Dec 2009, wind speed RMSE & bias 71

A-15: Jan 2010, wind speed RMSE & bias 72

A-16: Nov 2009, temperature RMSE & bias 72

A-17: Dec 2009, temperature RMSE & bias 73

A-18: Jan 2010, temperature RMSE & bias 73

LIST OF SYMBOLS

Symbol Page

A: area swept by wind turbine rotor blades 3

C_p: specific power coefficient for a turbine 3

D_1: domain one 42

D_2: domain two 42

D_3: domain three 42

D_i: larger domain 38

D_{i+1}: nested domain 38

d_{ij}: the difference between H_{ij} and G_{ij} 40

E_{ij}: root mean squared error 39

G_{ij}: estimate for the RMSE equation in the larger domain 39

H_{ij}: nested domain simulated wind speed 39

i^{th}: latitudinal index 26

j^{th}: longitudinal index 26

P: Power 3

p: pressure 14

Q: energy 1

q: water vapor 15

R: correlation coefficient 44

ρ: density of air 3

T: temperature 14

Symbol Page

U: wind velocity magnitude 3

$\bar{U}_{ij}$: average wind magnitude 26

u: zonal wind..... 14

u_{ij}: zonal wind 26

v: meridional wind 14

v_{ij}: meridional wind 26

w: vector wind..... 14

AFWA: Air Force Weather Agency..... 29

ARW: Advanced Research Solver..... 32

AWEA: American Wind Energy Association..... 7

CAPS: Center for Analysis and Prediction of Storms 29

CDAS: Climate Data Assimilation System 24

COAMPS: Coupled Ocean/Atmo Mesoscale Prediction System .. 12

ECMWF: European Ctr for Medium-Range Weather Forecasting 16

ESRL: Earth System Research Laboratory 29

EWEA: European Wind Energy Association..... 7

FAA: Federal Aviation Administration 29

FDDA: Four Dimensional Data Assimilation 31

FDE: finite difference equation 15

GDAS: Global Data Assimilation System..... 32

Symbol Page

GFS: Global Forecast System 32

GTS: Global Telecommunications System 32

GWEC: Global Wind Energy Council 4

LIDAR: light detection and ranging 18

MM5: Mesoscale Model 11

MMM: Mesoscale and Microscale Meterology Division 29

MYJ PBL: Mellor-Yamada-Janjic Planetary Boundary Layer 31

NCAR: National Center for Atmospheric Research 11

NCEP: National Center for Environmental Prediction 9

NCEP FNL: NCEP Final Analysis 9

NGSST-O: New Generation Sea Surface Temp for Open Ocean 31

NMM: Nonhydrostatic Mesoscale Model 32

NOAA: National Oceanic and Atmospheric Administration 29

NRL: Naval Research Laboratory 29

NWP: numerical weather prediction 11

NWS: National Weather Service 16

PBL: Planetary Boundary Layer 31

RAMS: Regional Atmospheric Mesoscale Model System 11

RRTM: Rapid Radiative Transfer Model 31

RMSE: root mean squared error 39

UCAR: University Corporation for Atmospheric Research 28

Symbol Page

WRF: Weather Research and Forecasting 9

WSF: WRF Software Framework..... 30

WSM3: WRF Single Moment 3-Class 31

WWEA: World Wind Energy Association..... 4

Chapter 1

INTRODUCTION

1.1 Wind Energy

Most forms of energy on Earth are derived from the sun. Wind energy is especially linked to the energy emitted by the sun. The sun, at its current evolution, emits $Q = 3.87 \times 10^{26}$ Watts (W) of energy. The Earth receives 1.74×10^{17} W of the energy emitted by the sun (Marshall & Plumb, 2008). This solar energy heats separate parts of the Earth's surface at different rates. For example, oceans and continents absorb and reflect solar energy at unequal rates. These varying rates of absorption and reflection cause portions of the atmosphere to warm differently. Warm air, being less dense, rises, which causes low pressure at the Earth's surface, see Figure 1.

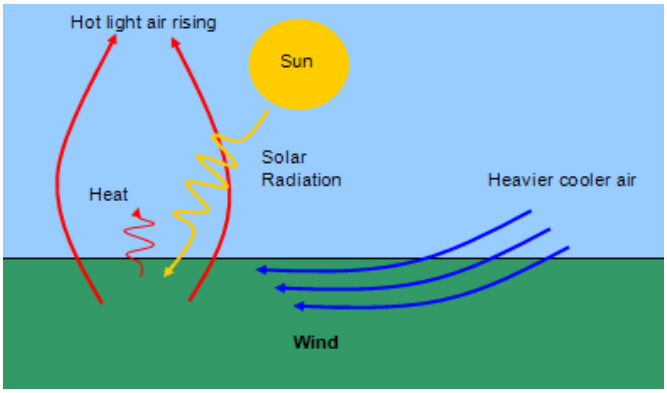

Figure 1: Wind illustration

Cold air moves from the more dense to less dense regions replacing the warm air at the Earth's surface. The result of this shift between more and less dense air is wind (Wind Energy, ERSU).

The atmosphere has mass, and mass in motion has kinetic energy. Wind is transportation of parcels of atmosphere and hence wind can be described as having kinetic energy. Wind energy can be effected by many different phenomena. Some of the most dominating phenomena that affect wind include: the Coriolis force (caused by the Earth's rotation), seasons (caused but the Earth's rotational axis being tilted relative to its orbital plane), and obstacles or surface roughness (such as mountains, cities, and vegetation). Exploiting all the free kinetic energy now contained within wind then becomes the objective of a mechanical system. This mechanical system's main objective is to convert wind energy into electrical energy (Parkinson K., 2001).

1.2 Wind Power Generation

Electricity is generated by converting the mechanical force exerted by wind on wind turbine rotor blades. The amount of energy converted into electricity depends predominately on wind

speed, density of air, and rotor area. There are more parameters to consider when trying to determine the power output by a single wind turbine; however, a quick approximation of the power generated by wind exerted on a wind turbine can be seen in Equation 1 (Kutz, 2007).

$$P = \frac{1}{2} C_p \rho A U^3 \quad (1)$$

In Equation 1, power (P) generated by a modern wind turbine is the product of the one-half the specific power coefficient (C_p) for that particular turbine, the density of air (ρ) passing through the turbine blades, the area swept by the rotor blades (A), and the wind velocity magnitude (U) of the air passing through the turbine cubed. Equation 1 illustrates the density of the air and the area swept by the rotor has a directly proportional effect on the power being generated. Yet, the power generated is effected by the cube of the wind velocity. This means if wind speed is doubled then the power generated is increased by a factor of eight (Parkinson, 2001).

Therefore the wind speed is the most important factor for determining how much energy is available to be turned into electricity. As the demand for electricity continues to increase more electrical power generation stations need to be

constructed. Because of this, wind energy generation is currently experiencing enormous growth. At the present, according to Nobel Environmental Power (2012), the fastest growing commercial-scale electric power generation in the United States is wind energy.

1.3 The Wind Energy Industry

Since the wind energy industry is currently experiencing a period of extreme growth research and resources have been concentrated on this topic. The growth, according to the World Wind Energy Association's (WWEA) annual "World Wind Report 2009," has caused the world-wide wind energy capacity to double in size every three years since 1992. The Global Wind Energy Council's (GWEC) "Global Wind Report 2011," communicated that even during the global recession, experienced in 2011, the world's wind energy capacity still increased by no less than 20.6%. The GWEC's report goes on to illustrate that of the 40.6 Gigga-Watts (GW) of the newly installed wind capacity China and the United States contributed the largest market shares, adding 43% and 17%, respectively in 2011 (GWEC, 2011). China's rise to the top of wind capacity installation has been swift. According to "Eco-Economy

Indicators" and an article by Matthew Roney, of the Earth Policy Institute, China's rise started when their installed capacity doubled in 2004 and continued to double every year until 2009. In 2010 China overtook the U.S. in total installed capacity (GWEC, 2011).

The market within the United States posted an annual growth in wind power of 30% during 2011. This growth signified an additional 6.810 GW for the country in that year. In total, forty-three states benefit from wind power; either directly through generating stations or indirectly by an increase in skilled-labor jobs through the manufacturing of turbines and turbine components. Of these states, thirty-eight benefit directly from wind power generation. The expectation is the industry will continue to grow during 2012. However, the Federal Production Tax Credit is set to expire at the end of 2012. This makes predictions into the 2013 market difficult to cast (GWEC, 2011). Considering all the growth in the U.S. industry and the expectation of continued growth worldwide, research in this field will contribute to the wind energy scientific community for years to come.

Significant amounts of research have been concentrated on determining offshore wind potential. Yet, the offshore

component of the installed capacity only represents approximately 2% of the global capacity. This begs the question: "Why are significant amount of resources being concentrated on offshore wind research when it appears to contribute so little to the global capacity?" Inherently, offshore wind potential has a greater ability to significantly reduce costs since wind speeds over water are generally greater than wind speeds over land. Wind speeds over water are greater due to very low surface reference length ($\approx 10^{-3}$-10^{-4} meters). In addition, offshore locations usually have a closer proximity to densely populated coastal regions, which can also contribute to lower costs. This is because being close to highly populated areas reduces transmission costs (GWEC, 2011).

1.4 Wind Farm Site Selection

When considering locations for potential wind farms several factors should be considered. Factors for consideration include availability of wind resources, revenue, costs, environmental and site access (Kutz, 2007). Offshore locations have significant available wind resources, as was noted above. However, high installation costs and difficult site access impede the construction of offshore wind farms. In fact, according to

the American Wind Energy Association (AWEA), the U.S. currently does not have any installed offshore wind farms. Only a hand-full of countries have offshore wind farms installed. The United Kingdom and Denmark are two of the largest contributors. The European Wind Energy Association (EWEA) predicts that by 2020 European Union investment for offshore wind farms will start to match the investments for onshore wind farms. Currently, the U.S. is behind in offshore capacity, as the U.S. has no offshore wind farms. Europe's heavy investment in offshore locations may have influenced the U.S. Department of Energy's recent creation of offshore wind farm incentives. These incentives may indicate the U.S. offshore market is on the precipice of significant offshore wind farm growth (Soren, K., Awerbuch S., & Monthorst, P. E., 2009).

As outlined in Section 1.2, wind speed is the most important parameter for converting wind energy into electrical energy. Due to this, it is logical wind farms should be placed at locations with high wind speeds. The most well-known ideal locations for wind farms are already being quickly converted into wind farms. Once all these known locations are developed the ability to determine new potential locations for wind farms will become increasingly more important.

1.5 Weather and Surface Wind Simulation

Determining potential ideal locations for wind farms involves an in-depth analysis which can include evaluating historical observed meteorological data, establishing an understanding of the laws within the state or in the international waters where a potential wind farm will be installed, and creating and analyzing a mesoscale meteorological model. This study will focus on evaluating availability of wind energy through the use of mesoscale meteorological modeling. Current available observed meteorological assimilation data is presented at a 1° × 1° grid resolution. This means the area being evaluated using observed meteorological assimilation data exclusively yields single grids with areas on the order of 10^5 kilometers squared (km^2).

1.6 Statement of Purpose

The surface wind profile at sub-grid resolution is completely unknown. Therefore to create a more refined surface wind profile at sub-grid resolution investigation using multi-scale nested grid resolution simulation was conducted. The investigation seeks to understand how changing grid resolution

impacts results. A Weather Research and Forecasting (WRF) simulation was conducted based off observed meteorological data assimilation datasets. The results contained within Chapter Four illustrate this extensive surface wind simulation. These high resolution surface wind simulations have a focus on both onshore and offshore locations. Current accepted wind simulation tools have varying accuracy and resolution length scales depending on the tool used. The WRF model was chosen because, according to the "Accuracy and Characteristics of Offshore Wind Speeds Simulated by WRF," an article written by Shimada and Ohsawa, the WRF model determines an annual positive correlation coefficient approximately 31% higher than current data assimilation observational datasets presented by the National Center for Environmental Prediction Final Analysis (NCEP FNL). The results contained within this document will demonstrate that grid resolution does impact the results of simulations and a positive difference at higher resolution will be found for offshore locations (Shimada & Ohsawa, 2011). This means a change in the grid resolution in the simulation (≈10-1000 meter squared) uncovers higher wind speeds than what is able to be ascertained from the current observed datasets and

accepted course resolution (≈1-2.5° square latitudinal and longitudinal) simulations.

Chapter 2

BACKGROUND LITERATURE

2.1 Simulation Tools and Techniques

To consider the large scale meteorological values a numerical weather prediction (NWP) tool must be utilized. These systems employ sophisticated computational numerical techniques to solve the variable that describes an atmospheric state. Some of the more common tools for understanding mesoscale meteorological states include using data assimilation or employing the use of a mesoscale meteorological modeling simulator. Data assimilation datasets are analyzed collections of millions of observational measurements to give a representation of a current atmospheric state. The fundamental weakness of the current data assimilation tools are very course grid resolution. Therefore data assimilation is more frequently used as the initial conditions and boundary conditions for mesoscale meteorological modeling software. Some of the more common mesoscale meteorological modeling software include: MM5 (Mesoscale Model) created by National Center for Atmospheric Research (NCAR) and Pennsylvania State University; RAMS (Regional Atmospheric Mesoscale Model System) created by

scientists at Colorado State University; COAMPS (Coupled Ocean/Atmosphere Mesoscale Prediction System) created by the Naval Research Laboratory, the WRF model, and others (Kalnay et al., 1996).

2.2 Mesoscale Meteorological Modeling

Mesoscale meteorology is the study of atmospheric phenomena that falls between the micro-scale, typically looking at small turbulent eddies, and the synoptic-scale, generally evaluating hurricanes and tropical storms. Mesoscale models can have a horizontal grid resolution ranging from as small as 1 km to as large as 100 km, with a special domain as large as 1000 km × 1000 km, and a vertical span from the Earth's surface through the troposphere and tropopause to the lower portion of the stratosphere. The temporal resolution for mesoscale meteorology can be as short as less than an hour or as long as several weeks (in order to accommodate the length of an entire weather event). Typical atmospheric phenomena evaluated at mesoscale include tornadoes, water-spouts, thunderstorms, squall-line, sea-land breeze, and mountain-valley breeze (Vincent, Draxl, & Neilsen, 2010).

Mesoscale research is particularly interesting because phenomena at this scale can directly impact human activities. The research in this field has grown considerably since the 1970s as a result of the significant advancements made in observational data collection tools and numerical modeling capabilities (Peike, 2002). Applications for mesoscale meteorology modeling, as they relate to wind energy, can include examining wind resources, determining the climate or maximum expected wind speed at a given potential wind farm site, short term weather prediction, predicting future wind variation, determining wind farm power production, and identifying maximum wind speeds. Additional applications, outside the scope of wind *energy*, can include predicting weather events surrounding wildfires, predicting shifts in wind direction, effects on aviation (such as determining which runways to use and prepare), search and rescue efforts, determining where survivors are likely to be found, and the natural transportation of air pollution.

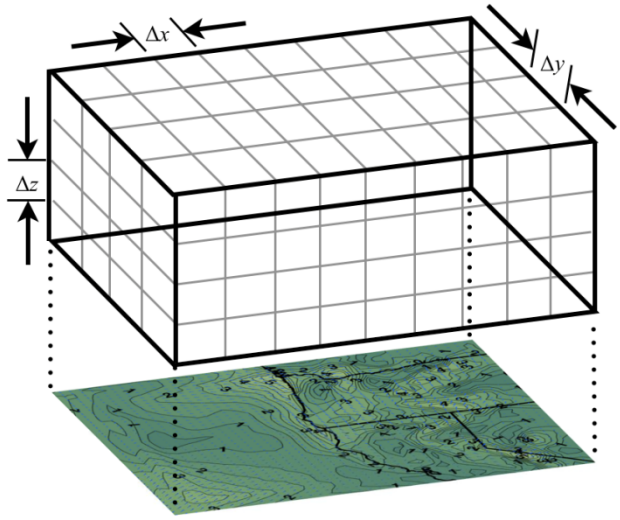

Figure 2: Mesoscale model 3D gridded domain

Mesoscale meteorological modeling works by generating a three-dimensional gridded domain over an area of interest, as seen in Figure 2, and applying discretized versions of the equations of motion for the atmosphere. The equations for motion within the atmosphere are derived from the ideal gas law and from the conservation principles of conservation of mass, conservation of heat, conservation of momentum, and conservation of moisture (seen in Equations 2-8; Pielke, 2002). The variables of interest that describe an instantaneous atmospheric state are zonal wind (u) or winds that move parallel to latitudinal lines, meridional wind (v) or winds that move parallel to longitudinal lines, vector wind (w) or winds that move normal to the Earth's surface, temperature (T), pressure (p),

density (ρ), and water vapor (q). As there are seven equations that describe atmosphere motion and seven variables of interest (u, v, w, T, p, ρ, q), then this system is considered closed and therefore solvable (Huang, 2011).

$$p = \rho RT \tag{2}$$

$$\frac{\partial p}{\partial t} = -\nabla \cdot (\rho \vec{u}) \tag{3}$$

$$Q = c_p \frac{dT}{dt} + \frac{1}{\rho}\frac{\partial p}{\partial t} \tag{4}$$

$$\frac{\partial u}{\partial t} = -\vec{u} \cdot \nabla u - \frac{1}{\rho}\frac{\partial p}{\partial x} - fv \tag{5}$$

$$\frac{\partial v}{\partial t} = -\vec{u} \cdot \nabla v - \frac{1}{\rho}\frac{\partial p}{\partial y} - fu \tag{6}$$

$$\frac{\partial w}{\partial t} = -\vec{u} \cdot \nabla w - \frac{1}{\rho}\frac{\partial p}{\partial z} - g \tag{7}$$

$$\frac{\partial q}{\partial t} = E - C - \vec{u}u \cdot \nabla q \tag{8}$$

To solve a mesoscale model the set of finite difference equations (FDEs) derived from the set of continuous differential equations, Equations 2-8, are used. Initial conditions and boundary conditions pulled from observational data assimilation datasets are imposed over the sets of FDEs solved simultaneously (Hoffman, K. A., & Chaing, S. T., 2004; Gilat, A., & Subramaniam, V., 2008). As stated earlier in Section 2.1, data assimilation datasets are analyzed collections of millions of

observational measurements. Data assimilation datasets are made available by the National Weather Service (NWS) and European Center for Medium-Range Weather Forecasting (ECMWF), and a complete explanation of how data assimilation datasets are generated follows in Section 3.2.2.

When considering mesoscale meteorological modeling it is important to understand the limitation inherent in the modeling. Mesoscale models cannot resolve small weather features that are approximately five times the horizontal length step or smaller (Vincent, Draxl, & Neilsen, 2010). Topographical and roughness features smaller than one horizontal length step will be "unseen" by the mesoscale model. This is troubling when considering course resolution mesoscale models could potentially not "see" entire mountain ranges, cities, or small forests. Mesoscale models are also limited by being unable to explicitly resolve turbulence. The results of mesoscale model can completely depend on the imposed initial and boundary conditions and rely on the accuracy of the input dataset. Mesoscale meteorological modeling also has a significant computational cost and is very time consuming. Another limitation is the probability of the occurrence of a specific given weather outcome cannot be determined from a single model. Therefore to determine the

likelihood of a specific outcome a set of mesoscale models must be generated.

2.3 Offshore Physics

The understanding that wind speed magnitude is higher over water than land is well known. As stated before, the sun heats the Earth's surface at different rates. During the day land warms more quickly than the nearby large bodies of water. This causes air to rise via natural convection. Cold, more dense, air parcels move from just above the large body of water to the less dense, lower pressure location over land. This process is then flipped during the evening. Large bodies of water resist drastic temperature changes while land areas cool quickly.

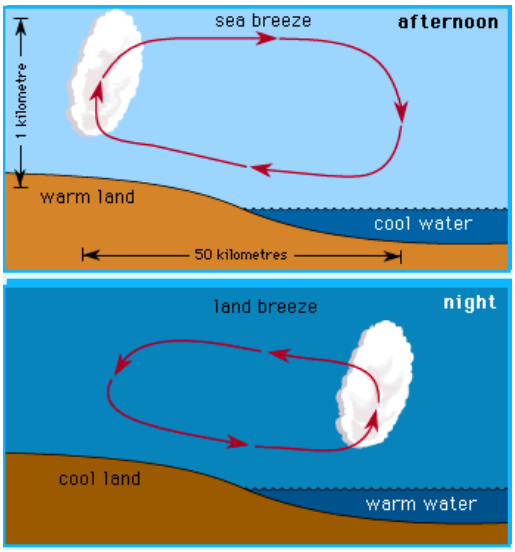

Figure 3: Sea-land breeze illustration

An air parcel, driven by the same natural convection principle, will then move from the more dense area over land to the less dense area over water (Poynting & Thomson, 1906).

Some of the difficulty with estimating offshore wind comes from the few numbers of sensing equipment and the complex dynamics from the sea-land breeze (Ohsawa, T., Hashimoto, A., Shimada, S., Yoshino, J., De Paus, T., & Heinemann, D., et al.,2007). The offshore wind dynamics could be even more complex when considering the cumulative wind speed of natural convection and gas exchanges over water (Olsen, A., Wanninkhof, R., Trinanes, J. A., & Johannessen, T., 2005).

Currently, there are large research projects to determine the amount of wind resources available. Some of the most high resolution empirical results come from LIDAR (light detection and ranging). LIDAR is a remote sensing system that transmits an eye-safe infrared laser beam. The infrared light goes out and senses aerosol scattering targets. To utilize this technology for offshore locations, the LIDAR system is first mounted to a boat. Then the vessel cuts zig-zags through the water (Pichugina, Y., Banta, R. Brewer, A. Hardesty, M., & Sandberg, S.). The results give very high resolution wind field data, but the range of field is limited. The need for mesoscale meteorological modeling and

simulation is therefore required to reduce the area of investigation.

Chapter 3

METHODOLOGY

3.1 Experiment and Simulation Overview

Section 1.5 stated that at high resolution offshore surface wind simulations illustrate the existence of a positive difference of the wind speed at offshore locations. In order to achieve an evaluation of wind speeds at higher resolution (to test for this positive difference), domains were nested within an existing resolution made available by the simulation.

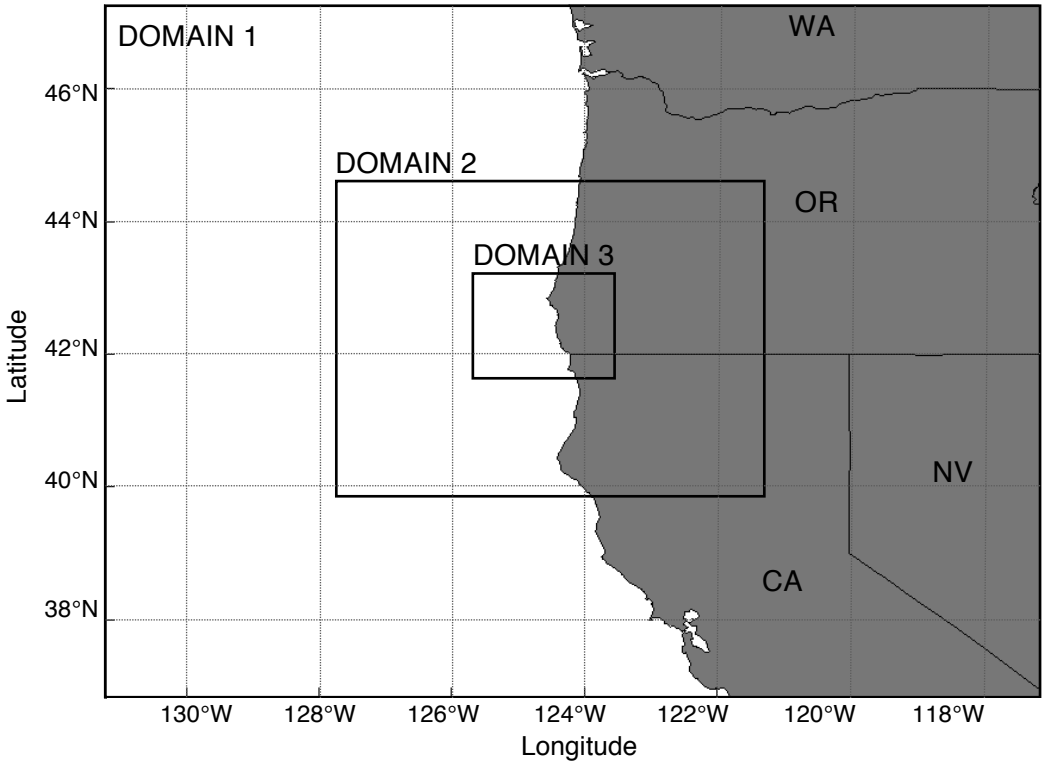

Figure 4: WRF simulated domains

Figure 4 illustrates Domain 1 as the available resolution and Domains 2 and 3 as the nested domains offering higher resolution. As the nested simulations are only more refined calculations of the larger domain in which they exist, then the simulations should be roughly the same. Therefore, wind speeds identified within Domain 3 should not be found to be drastically different than those observed over the same region from data collected at the resolution of Domain 1. The simulations were executed utilizing the Weather Research and Forecasting (WRF) model, version 3.2. The analysis conducted utilized these multiple layers of nested domains. The options within the WRF model allowed for increasing grid resolution which enabled a hindcast meteorological analysis for Domains 1, 2 and 3.

The investigation started with a cursory mesoscale surface wind analysis utilizing the National Center for Environmental Prediction (NCEP) and National Center for Atmospheric Research Reanalysis, a data assimilation, dataset. Atmosphere data assimilation is a dataset yielding an estimate, referred to as an "analysis," of a given historical meteorological state. An analysis using a data assimilation tool was done to identify an ideal location and period to be analyzed by the WRF model. After identifying an ideal location and time period, the WRF model, a

mesoscale meteorological modeling program, obtained real observational data from the National Centers for Environmental Prediction Final Operational Global Analysis (FNL) data. This is another data assimilation dataset with higher horizontal length grid resolution, which was used to execute the multi-resolution nested simulations for the domains of interest. The NCEP FNL Analysis data was used as the input for the WRF model. This WRF model created smaller higher resolution nested domains by imposing the results from the next larger domain as the boundary conditions for the next nested domain. The smaller domains were then solved for by utilizing the boundary conditions and the input data from NCEP FNL as well as the solution generated in the next larger domain in the WRF simulation. The results from the WRF simulation follow in Chapter Four.

3.2 Selection of Location to Examine

As the areas of the current observational data sets are so large ($\approx 10^5\,km^2$) potential consistent high magnitude wind velocity locations large enough to support a wind farm ($\approx$1-30 km^2) would never be identified (refer to Secs 1.5 and 2.2). Mesoscale meteorological modeling must be applied to an

observational set to achieve resolution in the surface wind velocity profile to help identify potential wind farm locations. Section 1.5 argues the existence of a positive difference at offshore locations between nested higher grid resolution simulations. As discussed in Section 1.2, the most important variable for converting wind energy into electrical power is wind velocity. If stronger winds exist offshore then selecting a potential wind farm site offshore would be ideal.

Light (1.6 m/s - 3.4 m/s) and gentle (3.4 m/s - 5.4 m/s) breezes, as defined by the Beaufort empirical wind measurement scale, are common types of wind, while moderate (5.5 m/s - 7.9 m/s), fresh (8.0 m/s - 10.7 m/s), and strong (10.8 m/s - 13.8 m/s) breezes are rare but highly desirable at wind farm locations. Hence, a location that contained great variation in wind speed magnitude was considered. Comparison of the results from course and fine resolutions simulations where there is significant wind speed variation will communicate the results are consistent no matter the magnitude of the wind speed within a given domain. The fine resolution simulation will undoubtedly have greater local maxima and smaller local minima than a course resolution simulation. A course resolution mutes the local extremas during the interpolation of the gridded results. To

ensure that the magnitude of wind does not influence the results a location that contains a broad spectrum wind speed magnitudes was chosen. This location was determined to be near the border between California and Oregon, just offshore.

3.2.1 Initial Analysis NCEP/NCAR Reanalysis

To identify a location for the study, a cursory analysis utilizing NCAR/NCEP Reanalysis, an analysis and forecasting system, that is also used for data assimilation, was employed (Kalnay et al., 1996). The NCEP/NCAR Reanalysis Project is a collaborative project between the National Center for Environmental Prediction and the National Center for Atmospheric Research. The objective of this project is to produce new atmospheric analyses using historical observational data starting in 1948 and continuing on until present. This project also seeks to produce analyses of the current atmospheric state for the Climate Data Assimilation System (CDAS). The variables that were used to generate the plots seen in Figure 5 were derived from the zonal wind and meridional wind.

a) Nov 2009

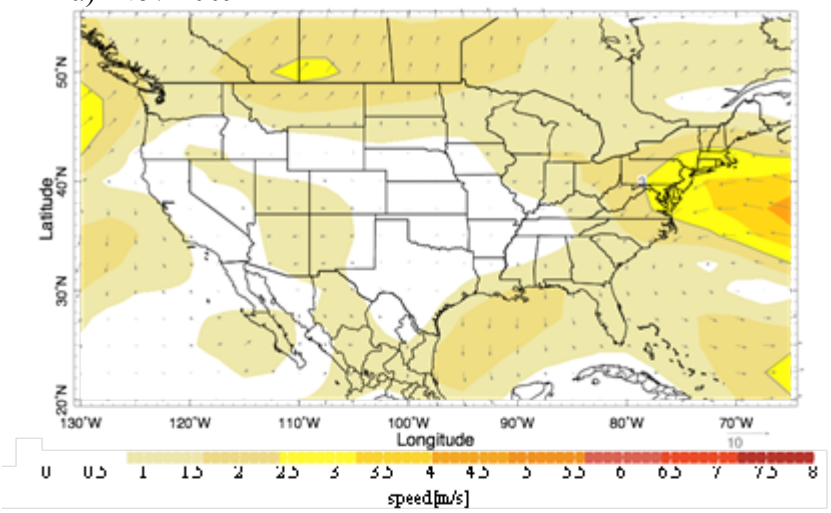

b) Dec 2009

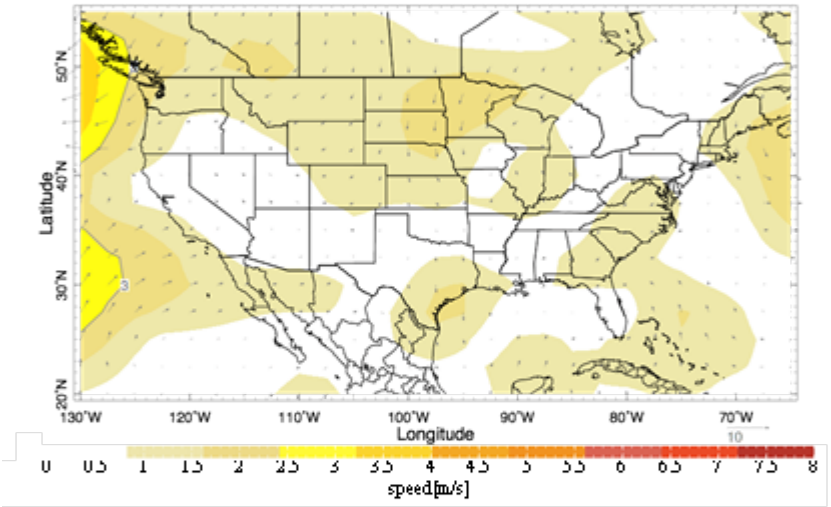

c) Jan 2010

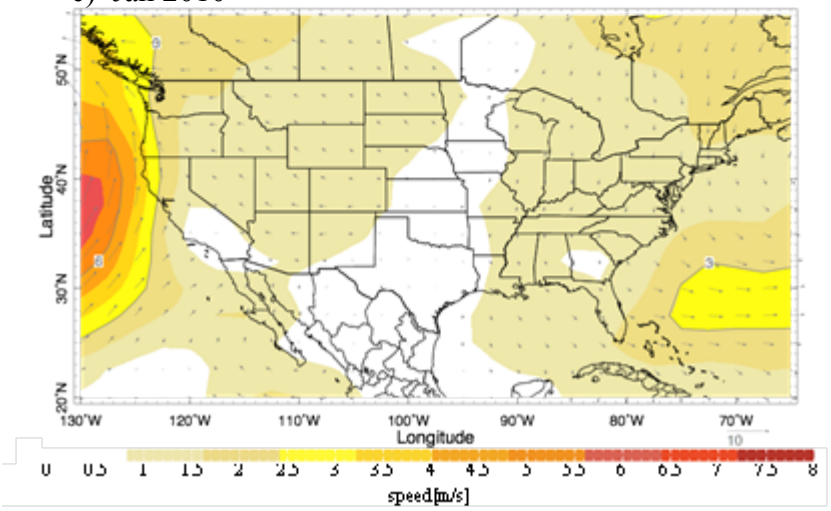

Figure 5: Reanalysis plots - site selection

These variables were presented by NCEP/NCAR Reanalysis at the 2.5° x 2.5° latitude and longitude grid resolution and considered at the 1000 mbar pressure level, or approximately the Earth's surface. The temporal resolution of the data contained within the Reanalysis dataset is six hours. Monthly averages were generated by the equation below, Equation 9.

$$\bar{U}_{ij} = \frac{1}{N}\sum_{n=1}^{N}\sqrt{u_{ij}^2 + v_{ij}^2} \quad \textbf{(9)}$$

In equation 9, ($\bar{U}_{ij}$) represents average wind magnitude, (u_{ij}) represents zonal wind, and (v_{ij}) represents meridional wind all at given i^{th}, latitudinal index, and j^{th}, longitudinal index, location. Equation 9 was applied to NCEP/NCAR Reanalysis datasets over the period of 2007-2011. The results demonstrated that, across the United States, the windiest seasons were winter and spring. The NCEP/NCAR Reanalysis was used because of the cheap computational cost of analysis.

The plots presented in Figure 5, illustrate the Reanalysis results for the entire duration of the higher resolution simulations executed by the WRF model. The offshore location near the state boundary between California and Oregon over the months of November 2009 through January 2010 was chosen to be evaluated. This location and time period yield a spectrum of

wind speed magnitudes to be analyzed and therefore was ideal for the multi-resolution, nested simulation.

3.2.2 Data Assimilation

Atmospheric data assimilation is created through a series of steps starting with the collection of millions of atmospheric conditions observed at weather stations at given time intervals, typically every six hours. The observations from weather stations all around the world are combined and analyzed to produce the analysis. The set of observations usually consist of several different measurement types, each having different accuracies and distributions. While the sets of observations are combined, specific consideration is given to accuracy and distribution of the meteorological variable observed at a given weather station. The analysis compilation is complete in terms of the domain, meteorological variables, and resolution. There is still a need to evaluate previous analyses to generate a complete representation of the current analysis. All analyses exist in a specific sequence and therefore a need to consider the proceeding analyses to develop the "background" in order to complete the current analysis. The background analysis carries

forward in time and spreads in space the information from the observations used in earlier assimilation cycles.

The observations and background are amalgamated using statistically based estimates of their errors. Variation assimilation integration of observed data and background information is achieved by minimizing the sum of error-weighted measures of the deviations of analyzed values from the observed and background values. The resulting sequence of initial states provides a record of the evolving atmospheric state that is based on a synthesis of the available observations; it depends implicitly on the dynamics and physics of the background analyses and on the error statistics. The degree to which an analysis depends on the background model varies with the density and relative accuracy of observed data. As weather stations are not uniformly distributed across the planet and the accuracy of a given weather station varies from station to station the dependence on the background varies from place to place and variable to variable. A complete analysis generated by the NCEP is then made available. This dataset is then presented by the NCAR data support section and made available to the research community via the University Corporation for Atmospheric Research (UCAR) website.

3.3 WRF Model

As discussed in Section 3.1, a thorough surface wind analysis was conducted utilizing the Weather Research and Forecasting model. The WRF model is a numerical weather prediction and atmospheric simulation tool. This tool is specifically designed as a mesoscale weather forecasting and data assimilation system used for research or operational weather forecasting (Michalakes *et al.,* 2001). The Weather Research and Forecasting model was developed by multiple agencies and universities including: National Center for Atmospheric Research, Mesoscale and Microscale Meteorology (MMM) Division, the National Oceanic and Atmospheric Administration (NOAA), National Center for Environmental Prediction, Earth System Research Laboratory (ESRL), the Department of Defense's Air Force Weather Agency (AFWA), Naval Research Laboratory (NRL), the Center for Analysis and Prediction of Storms (CAPS) at the University of Oklahoma, and the Federal Aviation Administration (FAA), as well as many other participating university scientists. The WRF model is capable of executing high level weather forecasting and simulation of three-dimensional variables such as: wind velocity profile, pressure,

temperature, precipitation, and potential temperature, among others. This tool was used specifically to simulate only the surface wind velocity profiles at higher resolution. As this program does not have the ability to solve one variable of interest the simulation recorded all the variables that describe an atmospheric state over the duration of the simulation.

3.3.1 WRF Model Software Structure

Numerical weather prediction software is only as accurate as the solvers that drive the model and the inputted initial and boundary conditions imposed. To develop an understanding of the WRF Software Framework (WSF), Figure 6 illustrates how input, such as data assimilation observational datasets or proceeding WRF simulations, interfaces with the solver and physic packages. The output results can then be used as the initial and boundary conditions for the next nested domain or be plotted and evaluated.

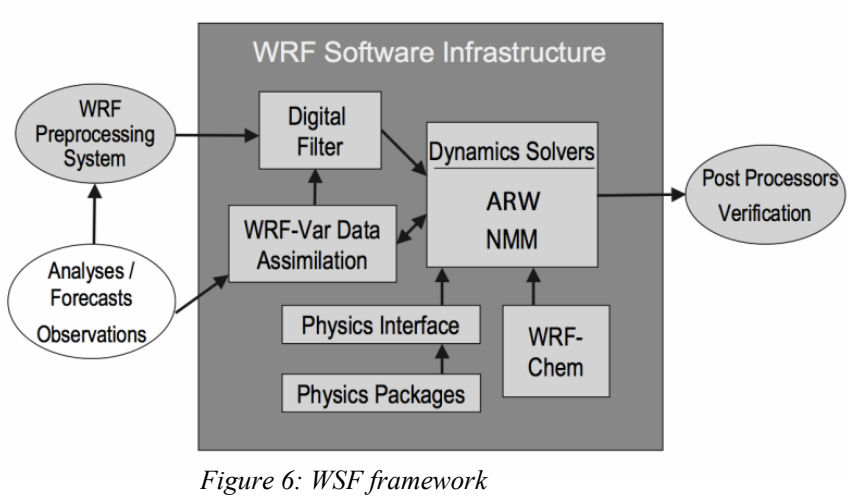

Figure 6: WSF framework

WRF Simulation Configuration	
Period	Start: 00:00 UTC 01 Jan 2009 End: 24:00 UTC 31 Jan 2010
Input Data	NCEP FNL Analysis (6-houlry, 1°×1°) NGSST-O (dailv. 0.05°×0.05°)
Nesting	3-Layer Nesting with Feedback
Domains	Domain 1: 27 km (44 × 44 grids) Domain 2: 9 km (60 × 60 grids) Domain 3: 3 km (60 × 60 grids)
Vertical Layers	28 levels (surface to 50 hPa)
Physics Options	-Dudhia Short Wave Radiation -RRTM Long Wave Radiation -WSM3 Cloud Micropysics -Kain-Fritsch 2 Cumulus Parameterization (for domains 1 & 2) -Five-Layer Soil Model -MYJ PBL Parameterization
FDDA Option	Enable excluding domains 2 and 3 PBL

Table 1: WRF simulation setup summary

The two dynamic solvers that exist within the WSF of the WRF model are the Advanced Research WRF (ARW) solver, the Eulerian mass solver (developed mostly at NCAR), and the Nonhydrostatic Mesoscale Model (NMM) solver (developed at NCEP). A summary of the WRF model with the selected/specified configurations can be seen in Table 1.

3.3.2 NCEP FNL Analysis Input Data

As stated earlier, the National Center for Environmental Prediction Final Operational Global Analysis data is a data assimilation project. It was also stated in Section 3.1 that the input observational data obtained for the WRF model simulation was from the NCEP FNL data assimilation project. The NCEP FNL analysis data is a dataset containing meteorological variables prepared on a 1° x 1° latitude and longitude grids with a six hour temporal resolution. This NCEP FNL product is from the Global Data Assimilation System (GDAS), which continuously collects observational data from the Global Telecommunications System (GTS), and other sources, for analyses. The FNLs are made with the same model which NCEP uses in the Global Forecast System (GFS).

3.4 Methodology Summary

The method utilized for the research conducted centered around utilizing available environmental research data to conduct a mesoscale meteorological model. The initial research used only NCEP/NCAR Reanalysis data assimilation datasets to select a site and time frame to investigate. This was followed by a multi-resolution nested simulation done by the WRF model, version 3.2. The NCEP FNL data assimilation datasets, the higher resolution datasets, were used to impose initial and boundary conditions on the WRF model simulations. The WRF model simulations have a high computational cost and the results took approximately three weeks to solve. The body of the analysis conducted, primarily presented in Chapter Four, was gleaned through post processing and validation process of the 100 gigabyte output file generated by the WRF model.

Chapter 4

DATA ANALYSIS AND RESULTS

4.1 WRF Model Results

The analysis from the first and largest domain can be seen in Figure 7. The most important observation that can be ascertained from these plots is how drastically different the surface wind magnitude appears for each month. This will provide sufficient variation for comparison. As the vector field communicates, magnitude is not the only parameter changing from month to month. The direction of the surface flow varies drastically as well. Demonstrating that these surface wind conditions are so dissimilar becomes increasingly more important when the comparison between plots yields similar results. In further investigations, specifically those for Domains 2 and 3, the vector fields were removed. This was done since the increased quantity of vectors started to occlude the plots as the grid resolution was increased. Figure 8 illustrates the highest resolution domain considered, Domain 3. It is also important to know that steep contour gradients can now to be observed in Figure 8. The contours are creating a stark separation in the area just offshore. It is important to note a noticeable grid-like

structure to that separation boundary.

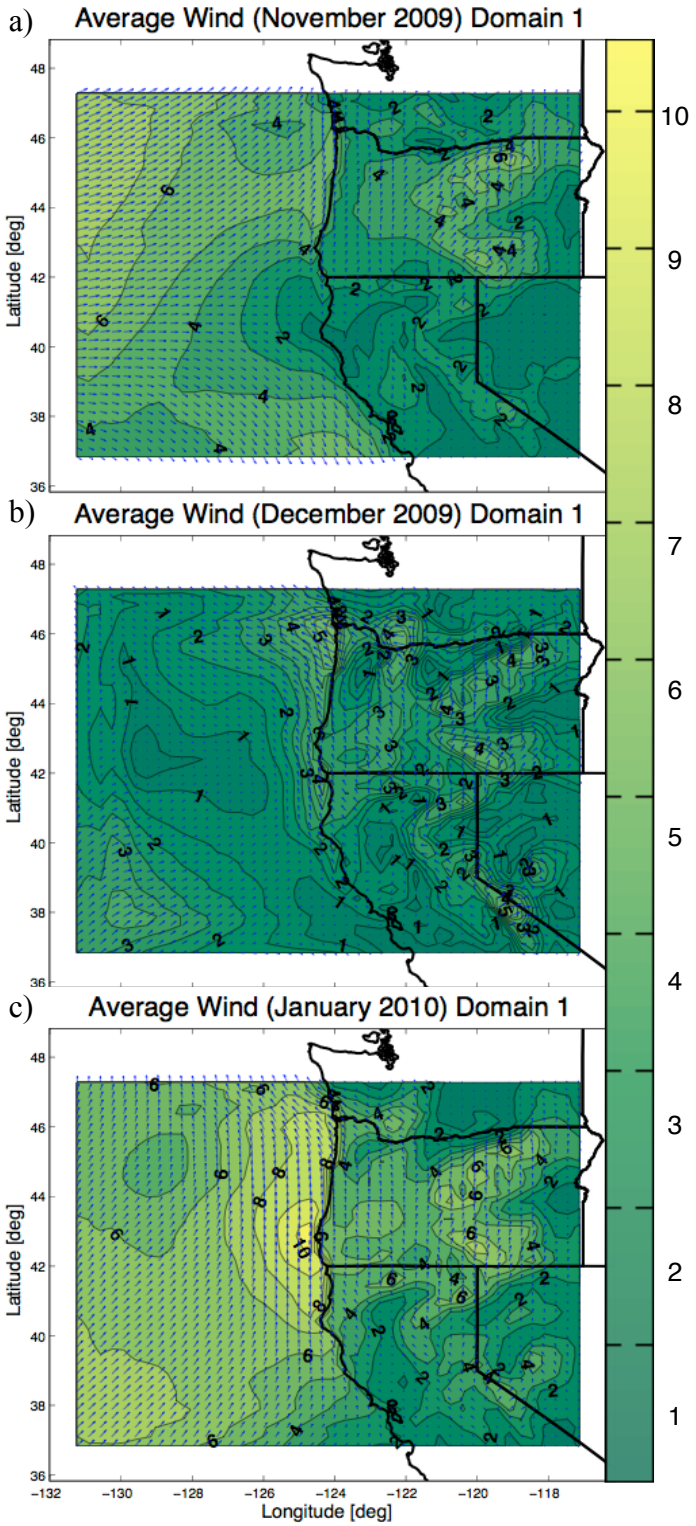

Figure 7: WRF domain 1 - wind speed plots

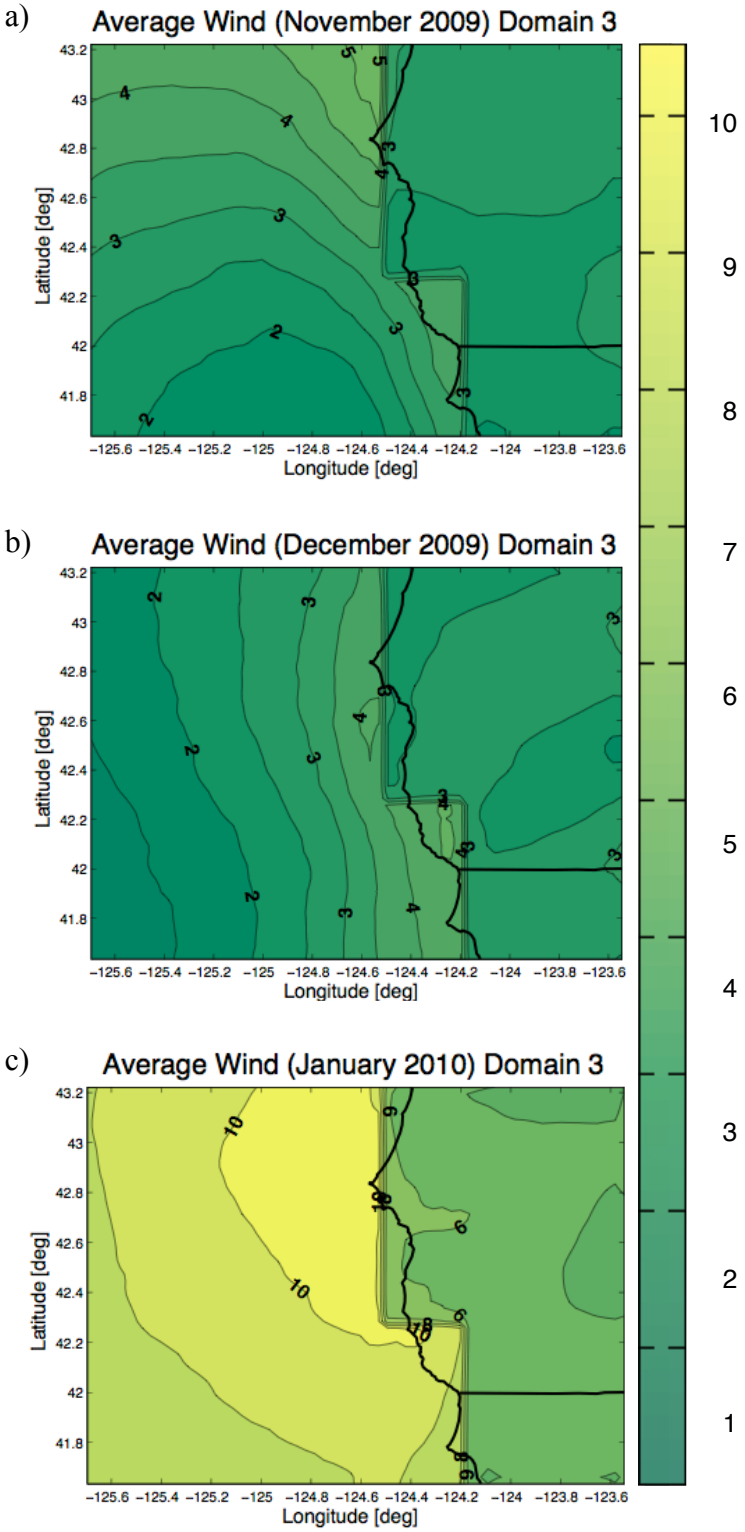

Figure 8: WRF domain 3 - wind speed plots

The reason for this grid-like separation between land and ocean was due to an option selected within the WRF simulation model. A limitation highlighted in the Mesoscale Meteorological Modeling section (Section 2.2) communicated that topographical features are usually lost as the observed scale grows smaller than the grid resolution. The topographical resolution could have been increased with each nested domain. Yet, since the analysis seeks to demonstrate how offshore wind magnitude is impacted by the simulation's solution grid refinement, topographical grid resolution was kept constant, and only the simulation solution grid was increased.

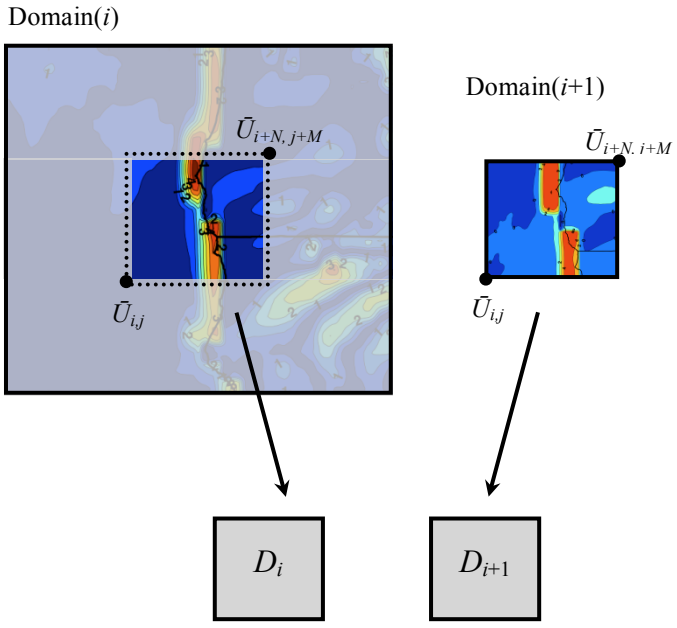

Figure 9: "Whole domain" comparison model

4.2 Domain Comparison

In order to compare the results from the domains side by side, plots were created. A subset of the larger domain was selected in such a way to align the latitudes and longitudes of the larger domain (D_i) and the a given nested domains (D_{i+1}). Figure 9 illustrates how each i^{th} and j^{th} average wind from D_i corresponds to the each i^{th} and j^{th} average wind from D_{i+1}.

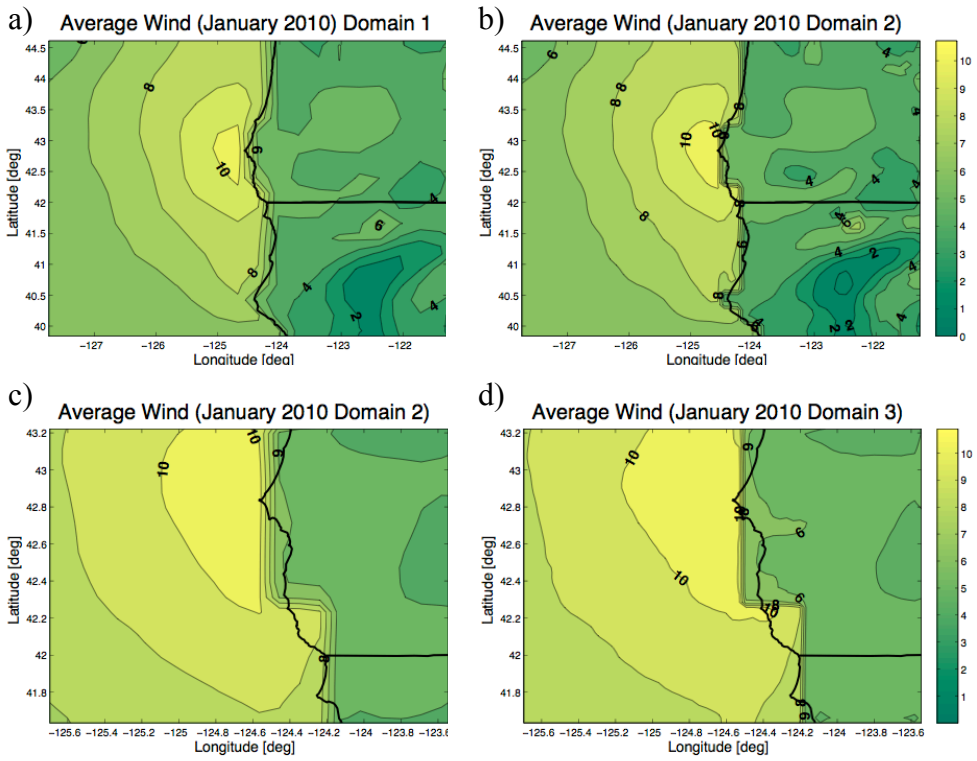

Figure 10: January 2010 side by side domain comparison

Figure 10 illustrations side by side allow qualitative analysis. This figure is useful for illustrating the point made in Location Selection (Section 3.3). This section argued that local

maxima and minima would be "higher" and "lower," respectively, at the domains of higher resolution. The month shown in Figure 10 is January 2010. All the side by side comparisons for the other two months also illustrate similar results and can be seen in Appendix A.

4.3 Offshore Wind Magnitude Bias

To quantify the amount of change from D_i to D_{i+1} additional results were generated. The results from Figure 11 a) was generated by taking the root mean squared error (RMSE) of the difference between D_i and D_{i+1}, seen in Equation 10. In Equation 10, (E_{ij}) represents the RMSE, $H_{ij} = \bar{U}_{ij}$ in the nested domain simulated wind speed results, and $G_{ij} = \bar{U}_{ij}$, commonly referred to as the estimate for the RMSE equation, within the next larger domain. This measure of error has units of m/s and will yield magnitude of error.

$$E_{ij} = \sqrt{\left(H_{ij} - G_{ij}\right)^2} \tag{10}$$

The RMSE is frequently written as a percent, or unit-less form, by dividing the difference of H_{ij} and G_{ij} by the estimated solution, in this case G_{ij}. This was not done because at a given

i^{th} and j^{th} location there can exist a specific $\bar{U}_{ij}$ that could be very small.

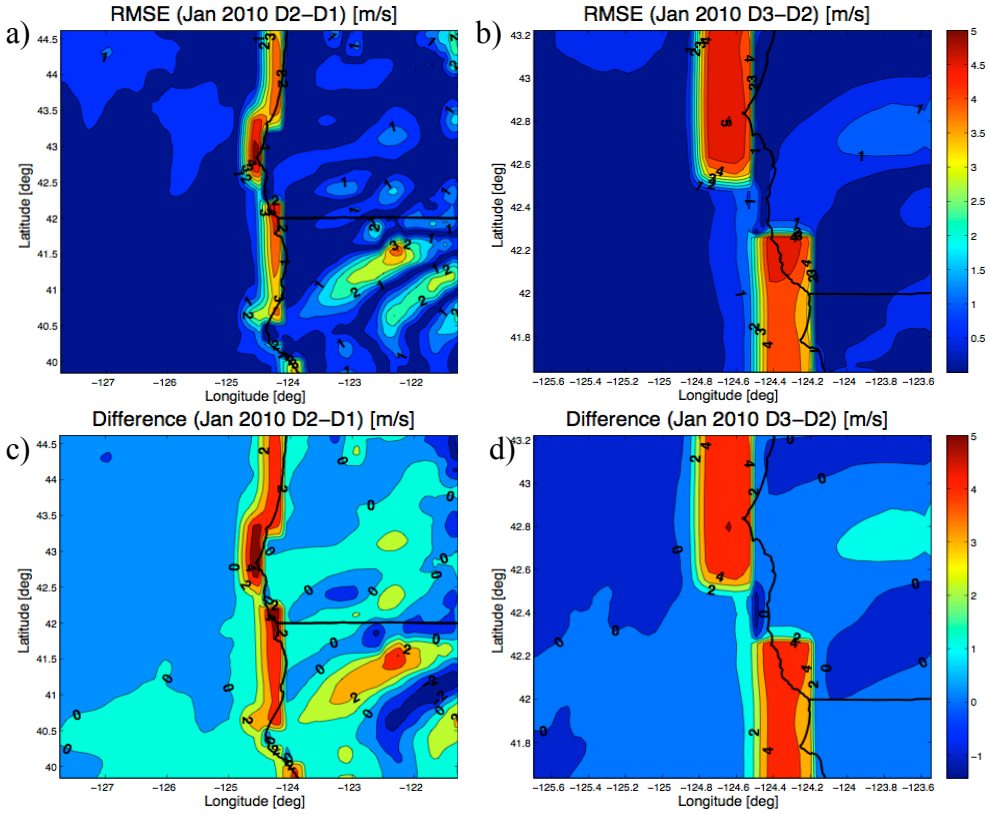

Figure 11: January 2010 RMSE and difference comparison

This will create conditions where singularities may arise and skew the results. Equation 11 illustrates another comparison tool utilized to compare the results from two domains.

$$d_{ij} = H_{ij} - G_{ij} \tag{11}$$

Equation 11 illustrates a simple difference equation where d_{ij} represents the difference of every H_{ij} and G_{ij} term the between any two domains, D_i to D_{i+1}. The units of this plot will

also have units of m/s. These differences will illustrate locations of where the results contained within D_{i+1} are either larger or smaller than the results contained within D_i. The month illustrated in Figure 11 is January 2010. All three months of RMSE and Difference plots yield similar results those presented in Figure 11 and Table 2.

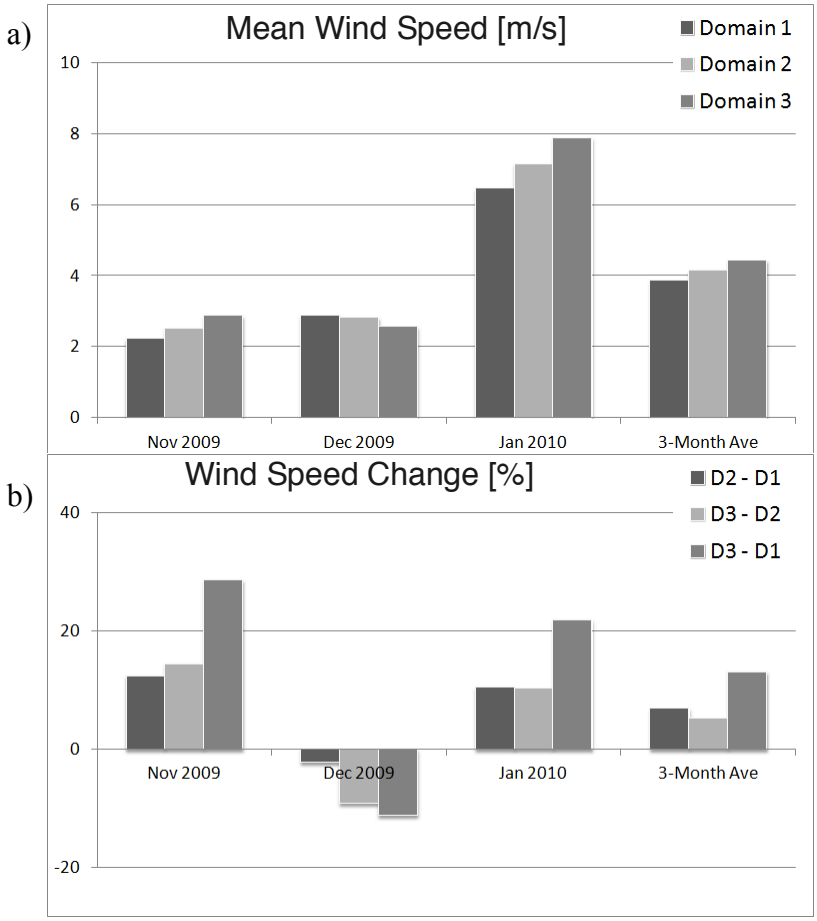

Figure 12: Whole domain mean wind speed statistics

Whole Domain

Time & Domain		Mean WS	STD [m/s]	$D_{i+1} - D_i$	Bias [%]
Nov 2009	D1	2.2292	0.5042	D2 - D1	12.39%
	D2	2.5055	0.6404	D3 - D2	14.40%
	D3	2.8663	0.7727	D3 - D1	28.58%
Dec 2009	D1	2.8825	0.4770	D2 - D1	-2.22%
	D2	2.8186	0.5976	D3 - D2	-9.15%
	D3	2.5606	0.7134	D3 - D1	-11.17%
Jan 2010	D1	6.4565	1.9580	D2 - D1	10.48%
	D2	7.1333	2.1522	D3 - D2	10.26%
	D3	7.8649	2.0754	D3 - D1	21.81%
	Ave D1	3.8561	0.9798	Ave D2 - D1	6.89%
	Ave D2	4.1525	1.1301	Ave D3 - D2	5.17%
	Ave D3	4.4306	1.1871	Ave D3 - D1	13.07%

Table 2: Whole domain wind speed statistics

As Figure 11 only allows a qualitative comparison between two given domains a statistical comparison was also conducted to provide a more complete description of the changes as grid resolution is increased. In Figure 12 a) illustrates the mean wind speeds as a given domain. The results of Figure 12 b) illustrate the percent change between any two domains. For example, the results present the percent change between domain two, D_2, and domain one, D_1, domain three, D_3, and domain two, D_2, and domain three, D_3, and domain one, D_1, respectively.

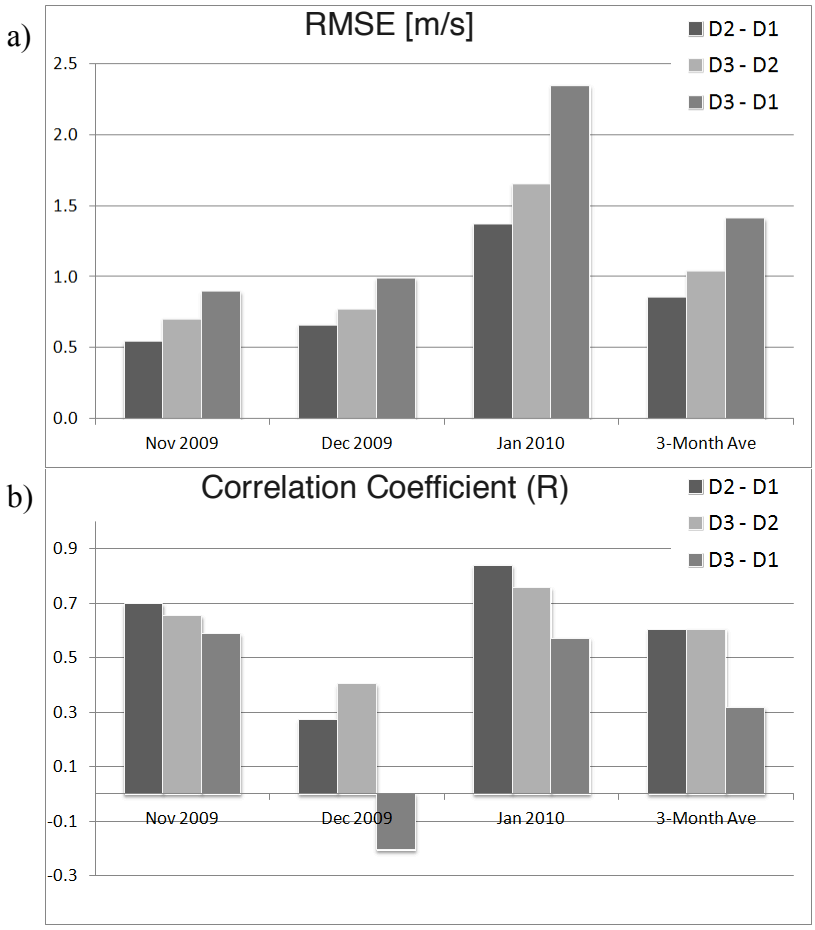

Figure 13: RMSE & correlation coefficient wind speed statistics

Whole Domain					
Time & Domain		**RMSE**	**STD [m/s]**	D_{i+1} - D_i	**Bias [%]**
Nov 2009	D1	0.5398	0.4176	D2 - D1	29.81%
	D2	0.7007	0.4677	D3 - D2	27.69%
	D3	0.8947	0.7663	D3 - D1	65.75%
Dec 2009	D1	0.6586	0.3232	D2 - D1	16.58%
	D2	0.7678	0.3565	D3 - D2	28.89%
	D3	0.9896	0.5252	D3 - D1	50.26%
Jan 2010	D1	1.3672	1.1153	D2 - D1	20.68%
	D2	1.6499	1.2957	D3 - D2	41.94%
	D3	2.3419	2.1258	D3 - D1	71.29%
	Ave D1	0.8552	0.6187	Ave D2 - D1	22.36%
	Ave D2	1.0395	0.7066	Ave D3 - D2	32.84%
	Ave D3	1.4087	1.1391	Ave D3 - D1	62.43%

Table 3: Whole domain RMSE & bias statistics

A statistical analysis was also done to investigate the RMSE and how close the wind speed results correlate to the wind speed magnitudes of another domain, both seen in Figure 13 and Table 3. The results presented in Figure 13 a) are the RMSE change between domain two, D_2, and domain one, D_1, domain three, D_3, and domain two, D_2, and domain three, D_3, and domain one, D_1, respectively. To determine the correlation between the any two domains the correlation coefficient equation, seen in Equation 12, was used (Bluman, 2001).

$$R = \frac{n\left(\sum G_{ij}H_{ij}\right) - \left(\sum G_{ij}\right)\left(\sum H_{ij}\right)}{\sqrt{\left[n\left(\sum G_{ij}\right) - \left(\sum G_{ij}\right)^2\right]\left[n\left(\sum H_{ij}\right) - \left(\sum H_{ij}\right)^2\right]}} \quad \textbf{(12)}$$

The correlation coefficient measures the strength and direction of the linear relationship that exists between two given data sets. Figure 14 b) is therefore useful at illustrating the similarity between the results of two domains.

4.4 Offshore Temperature Bias

The analysis investigated how offshore wind magnitude has been impacted by grid resolution. Results similar to those present in Figure 14, presenting RMSE and the difference between two domains, will be generated for temperature, a

different physical parameter. The surface temperature was solved along with the surface wind within the mesoscale modeling done by the WRF model. The results from this analysis can be seen in Figure 14.

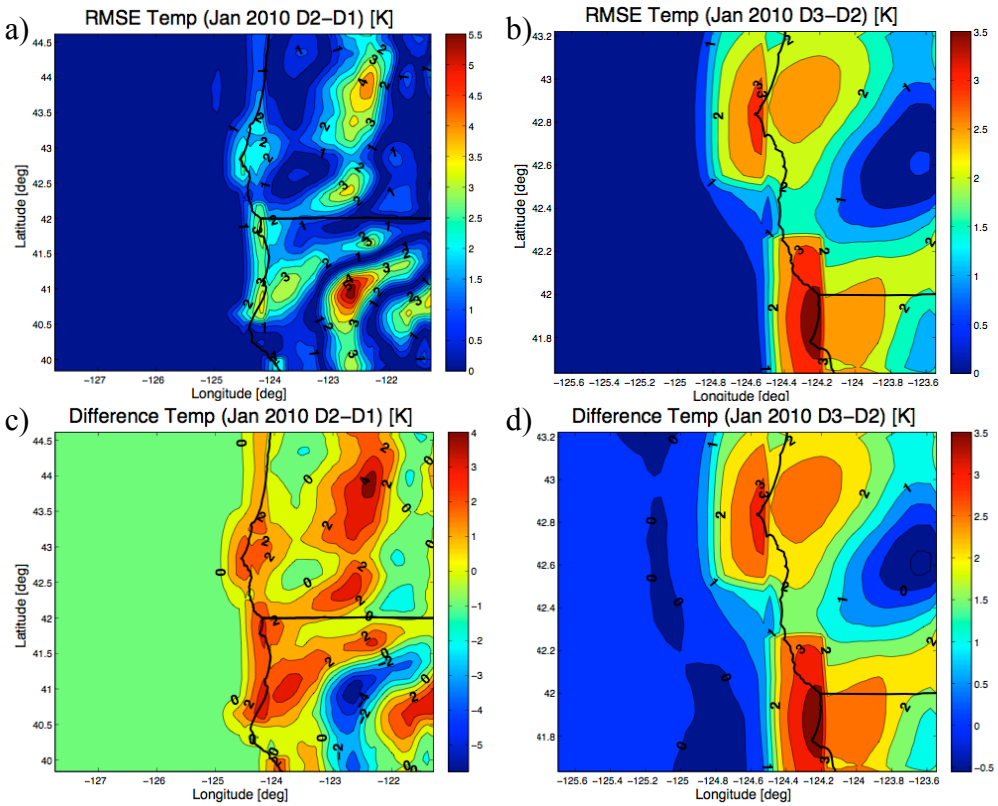

Figure 14: January 2010 RMSE and difference temperature comparison

Chapter 5

DISCUSSION

5.1 Examining Extrema through Grid Resolution

The study conducted, filtered, and compared significant amounts of data. One of the assumptions made in Section 3.2 was that at low resolution local maxima and minima are muted. Figure 10, illustrates this point well when looking at plots a) and b). There are several local maxima and minima missing from plot a) that are able to be observed in plot b) including minima at 122.5W, 40.75N and 123.25W, 42.5N, and maxima at 122.5W, 41.5N. A similar observation can be seen in plots c) and d) where d) illustrates a larger high value contour area at 124W, 42.2N than plot c). It is important to point out sub-grid process impact the results. A limitation outlined in Section 2.2 was that any meteorological phenomena that is on the spacial resolution of five to seven times the spacial grid size resolution would be unseen by the mesoscale meteorological modeling software (Vincent, C, Draxel, C, & Nielson, J, 2010). Those processes identified at the sub-grid scale influence the large scale flow of wind velocity profile and therefore cannot be ignored.

5.2 Implications of the Existence of Bias

The most interesting results generated during the course of this study came from the significant positive bias in surface wind speed magnitude identified just offshore in Figure 11 and in subsequent plots in Appendix A. Figure 7 is an illustration of how drastically different the surface wind speed magnitude and vector fields are for each month.

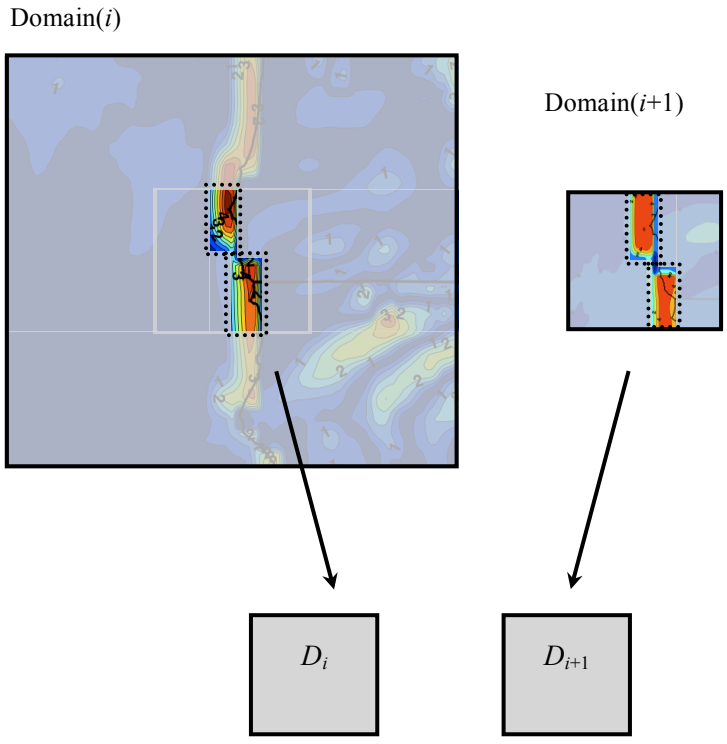

Figure 15: "Offshore domain" comparison model

The results contained within Figure 11 and those in Appendix A illustrate that even though the surface wind profile

experienced broad variation over the period analyzed, higher wind speed magnitudes were always identified at offshore locations. The identification of and location with consistent high wind speed is significant.

5.3 Statistical Analysis of Bias

To confirm the positive bias of offshore wind speed magnitude observed qualitatively a statistical analysis was done. The results contained in Figure 11 generally demonstrate that as grid resolution was increased so did RMSE and positive difference for wind speed magnitudes. One month, December 2009, did not follow this trend. The results of Figure 12 communicate the mean wind speed and the change from one domain to another. The results from the entire domain from December 2009 were included and therefore skewed all the results for the offshore locations of wind speed.

5.4 Narrowing the Scope to Offshore Locations

A further investigation only examined offshore locations. This was done by only analyzing the change at offshore locations, as illustrated by Figure 15. The results of the statistical analysis convey that offshore locations have higher

wind speeds when simulated at higher grid resolution. When only considering the offshore locations the wind speed always increased as grid resolution was increased. Figure 16 and Table 4 can be used to illustrate that the average expected increase in wind speed at offshore locations is 68.4%.

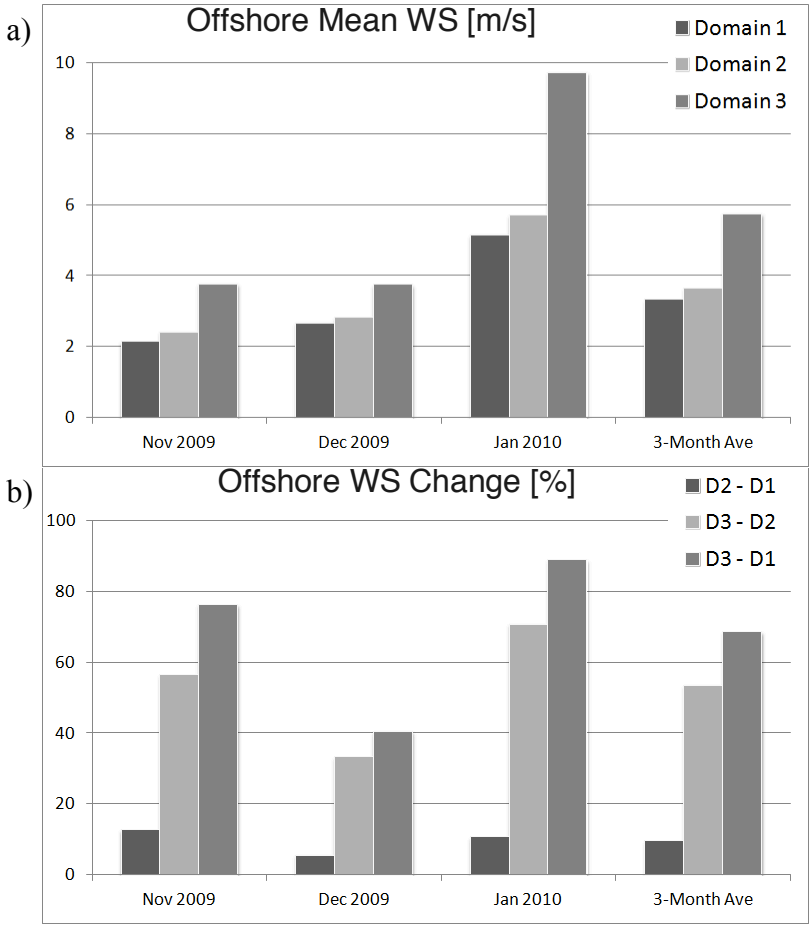

Figure 16: Offshore domain mean wind speed statistics

Offshore Domain					
Time & Domain		Mean WS	STD [m/s]	D_{i+1} - D_i	Bias [%]
Nov 2009	D1	2.1345	0.3795	D2 - D1	12.72%
	D2	2.4059	0.3724	D3 - D2	56.27%
	D3	3.7597	0.8284	D3 - D1	76.14%
Dec 2009	D1	2.6632	0.1613	D2 - D1	5.45%
	D2	2.8084	0.2643	D3 - D2	33.14%
	D3	3.7392	0.5184	D3 - D1	40.40%
Jan 2010	D1	5.1418	0.5295	D2 - D1	10.62%
	D2	5.6877	0.7256	D3 - D2	70.64%
	D3	9.7056	1.1038	D3 - D1	88.76%
	Ave D1	3.3132	0.3568	Ave D2 - D1	9.60%
	Ave D2	3.6340	0.4541	Ave D3 - D2	53.35%
	Ave D3	5.7348	0.8169	Ave D3 - D1	68.43%

Table 4: Offshore domain wind speed statistics

5.5 Domain Correlation

The domains are considered to be moderately correlated with three month averages of the correlation coefficients over 0.60. The only three month average correlation coefficient found to be low was that comparing D_3 and D_1. This low correlation coefficient was about 0.31, seen in Table 5. This is to be expected as each iterative nested simulation moves further away from the initial simulation. December was found to have a negative value for a correlation coefficient, when comparing the nested domains in that month. A possible reason for the

different results for December 2009 could be this month is generally considered a seasonally transitional month.

Whole Domain (WS)		
Time & Domain		**Corr. Coef.**
Nov 2009	D1	0.6957
	D2	0.6530
	D3	0.5859
Dec 2009	D1	0.2716
	D2	0.4022
	D3	-0.2050
Jan 2010	D1	0.8370
	D2	0.7558
	D3	0.5708
	Ave D2 - D1	0.6014
	Ave D3 - D2	0.6037
	Ave D3 - D1	0.3172

Table 5: Whole domain wind correlation

5.6 Examining Temperature

To further investigate how other physical parameters are impacted by grid resolution temperature was also considered. Figure 14 illustrates a positive bias at offshore locations for temperature; however, if the entire domains are considered it can be observed that that there are other locations with higher temperature changes. A statistical analysis was done resulting in 0.96, 0.93, and 0.86 correlation coefficients for domain two, D_2, and domain one, D_1, domain three, D_3, and domain two, D_2, and domain three, D_3, and domain one, D_1, respectively, seen in

Table 6. Correlation coefficients that close in value to 1 are considered very highly correlated. This means that temperature does not vary much as grid resolution is increased.

Whole Domain (Temp)		
Time & Domain		**Corr. Coef.**
Nov 2009	D1	0.9549
	D2	0.9329
	D3	0.8568
Dec 2009	D1	0.9560
	D2	0.9342
	D3	0.8627
Jan 2010	D1	0.9566
	D2	0.9242
	D3	0.8561
	Ave D2 - D1	0.9558
	Ave D3 - D2	0.9304
	Ave D3 - D1	0.8585

Table 6: Whole domain temperature correlation

Chapter 6

CONCULSION

6.1 Summary of Findings

This study sought to glean a better understanding of the grid resolution for a single variable within a set of multi-resolution nested simulations executed by the WRF model. The findings can be enumerated as follows:

1) The results for wind speed magnitude between a given domain and the next smaller nested domain change considerably. This result can be observed when considering the three month average correlation coefficient of 0.60 between Domains 1 and 2 and 0.60 between Domains 2 and 3.

2) The results for temperature between a given domain and the next smaller nested domain remain relatively unchanged. The three month average correlation coefficient for domain 1 and 2 was found to be 0.96 and 0.93 for domains 2 and 3.

3) The three month average mean wind speed over the entire examined domains increased by 13.1% from the most course grid resolution to the most refined resolution; however, if just the offshore locations within the domains are considered

a three month average mean wind speed increase by 68.4% from the most course grid resolution to the most refined resolution.

6.2 Implications of Findings

The implication of this research can drastically change how available wind energy is evaluated. The results illustrating a 68.4% increase of available wind speed over offshore locations would deliver over six times more power when considering the approximate electrical power from a wind turbine (Equation 1). As is demonstrated by the simulations, wind speed was found to be significantly more sensitive than temperature. This could indicate one of two conclusions should been drawn about why this was found to occur. 1) The WRF model is more accurate at determining actual wind speed than observational data assimilation is able to resolve. Or, 2) the WRF model fabricates the increase inherent to the solver and physics packages utilized. Depending on which one of these two possibilities is the true reason for the observed changes in wind speed, the way the WRF model is used to analyze weather patterns in the future could be drastically impacted.

6.3 Suggestions for Future Research

The work in this field will continue to grow as the demand for wind power continues to grow. Simulations augmenting current observational data assimilation datasets are becoming more common. As the simulations become more common a need to understand how the results are impacted by grid resolution also needs to develop. This study demonstrated when considering the parameter of surface wind speeds increases were observed at offshore locations when consulting higher grid resolutions. Since this research was limited to a three-month time span, conducting additional research is recommended in order to generate a complete picture of the accuracy of the simulation in regards to grid resolution.

Generating a better understanding of the accuracy and correlation of a simulation tool could be done by setting up an array of "*in-situ"* weather collection stations, over a large area ($\approx$ 100 km^2 - 1000 km^2), which matches the resolution (land area) of the smallest domain simulations. This would allow the WRF model or any other mesoscale meteorological modeling software to verify results of simulations at a higher resolution than what current accuracy rates provide. A study of the results gathered from these in-situ weather stations could also examine

how results are impacted by the input assimilation data used. Having the availability of this type of empirical study coupled with simulation tools will be instrumental in creating an understanding of how the results of next generation simulation tool, such as results generated by WRF, are impacted by parameterization.

Another potential avenue for improving the field of study within this scientific community would be to see how grid resolution impacts other parameters. The results of this study considered the possibly that the changes in wind speed magnitude were factitious and therefore investigated for similar fabricated results for temperature within the simulation. A full scale study should be conducted of how all the variables of interest are impacted by a change in grid resolution. This study would evaluate how the values of the parameters change as a result of grid resolution. These results would then indicate whether or not the increases observed through this document's study are valid or if they are simply the results always produced by the simulation no matter the parameter being observed. This indicates further investigation should be conducted to help determine if simulated results are real and not only observed due to a lack of weather sensing stations and temporal

resolution, or a fabrication of the simulation itself. A thorough investigation of how the mesoscale meteorological modeling software parameterizes data, conducts transformations, and applies physics packages and solvers should be conducted for the whole of the gridded domain.

As stated earlier, the field of mesoscale meteorological model field as grown considerably since the 1970s. This has happened due to the proliferation and advancements made in computing ability. The results for this study took around three weeks to compile, and this study was limited to only examining three months with the smallest domain span approximately 180 km × 180 km. The computer science software developers or hardware designers could create advancements in the computational solver field to assist in finding new ways of reducing the high computational cost as well as reducing the amount of time needed to run a full-scale analysis/simulation across certain areas. Both of these advancements would increase the potential for these simulation tools to be used to investigate the impacts of higher grid resolution over larger domains without consuming copious amounts of money and time. If identifying new potential locations for wind farms could benefit from studies at higher resolutions, then the industry

would also benefit by being able to utilize accurate simulation tools that are less expensive and faster.

6.4 Conclusion

This field of study still has much to investigate. Wind power generation and installed capacity has been growing at exponential rates since the early 1990s and does not appear to be slowing. Whether this field is improved through empirical *in-situ* validation, examining the entire scope of varying model parameterization and the impacts on simulated results, or creating new software or hardware there will continue to be a need for this type of research for years to come.

REFERENCES

Archer, C. L., Jacobson, M. Z., (2003). Spatial and temporal distributions of U.S. winds and wind power at 80 m derived from measurements. *Journal of Geophysical Research - Atmospheres, 108*(D9), 4289.

Baik, J., Park, S., & Kim, J. (2009). Urban flow and dispersion simulation using a CFD model coupled to a mesoscale model. *Journal of Applied Meteorology and Climatology, 48*(8), 1667-1681.

Barker, D. M., Huang, W., Guo, Y., Bourgeois, A. J., & Xiao, Q. N. (2004). A three-dimensional variational data assimilation system for MM5: Implementation and initial results. *Monthly Weather Review, 132*(4), 897-914.

Barthelmie, R. J., Courtney, M. S., Højstrup, J., & Larsen, S. E. (1996). Meteorological aspects of offshore wind energy: Observations from the vindeby wind farm. *Journal of Wind Engineering & Industrial Aerodynamics, 62*(2), 191-211.

Barthelmie, R. J., & Pryor, S. C. (2006). Challenges in predicting power output from offshore wind farms. *Journal of Energy Engineering, 132*(3), 91.

Beaudry-Losique, J., Boling,, T., Brown-Saracino, J., & et al. (2011, February). A national offshore wind strategy: Creating an offshore wind energy industry in the United States. *U.S. Department of Energy*, Retrieved from http:// www1.eere.energy.gov/wind/pdfs/ national_offshore_wind_strategy.pdf

Bluman, A. G., (2001). *Elementary statistics: A step by step approach* (4th Ed.). New York: McGraw-Hill Companies, Inc.

Colle, B. A., Olson, J. B., & Tongue, J. S. (2003). Multiseason verification of the MM5. part I: Comparison with the eta model over the central and eastern united states and impact of MM5 resolution. *Weather and Forecasting, 18*(3), 431-457.

Done, J., Davis, C. A., & Weisman, M. (2004). The next generation of NWP: Explicit forecasts of convection using the weather research and forecasting (WRF) model. *Atmospheric Science Letters, 5*(6), 110-117.

Donner, L. J., Seman, C. J., Hemler, R. S., & Fan, S. (2001). A cumulus parameterization including mass fluxes, convective vertical velocities, and mesoscale effects: Thermodynamic and hydrological aspects in a general circulation model. *Journal of Climate, 14*(16), 3444.

Gilat, A., & Subramaniam, V., (2008). *Numerical methods for engineers and scientists: An introduction with applications using MATLAB*. Hoboken: John Wiley & Sons, Inc.

GWEC (2011). Global wind report: Annual market update 2011. Retrieved from http://www.gwec.net/fileadmin/documents/NewsDocuments/Annual_report_2011_lowres.pdf

Hodur, R. M. (1997). The naval research Laboratory's coupled Ocean Atmosphere mesoscale prediction system (COAMPS). *Monthly Weather Review, 125*(7), 1414-1430.

Hoffman, K. A., & Chaing, S. T., (2004). *Computation Fluid Dynamics* (4th ed.). Wichita: Engineering Education Systems.

Huang, H. P., (2011, October). Geophysical and environmental fluid dynamics [course notes].

Kalnay et al., (1996). The NCEP/NCAR 40-year reanalysis project. *Bulletin of the American Meteorological Society*, 77, 437-470.

Krieger, J., Zhang J., Atkinson, D., Shulski, M., & Zhang, X. (2009). Sensitivity of WRF model forecasts to different physical parameterizations in the Beaufort Sea region. *Presented at the Eighth Conference on Coastal Atmospheric and Oceanic Prediction and Processes in Phoenix, AZ, January 12-15, 2009.*

Lo, J. C., Yang, Z. L. Yang, & Pielke, R. A. (2008). Assessment of three dynamical climate downscaling methods using the weather research and forecasting (WRF) model. *Journal of Geophysical Research - Atmospheres, 113*(D9), D09112.

Marshall, J., & Plumb, R. A., (2008). *Atmosphere, oceans, and climate dynamics: An introductory text*. Cambridge: Academic Press.

Mahrt, L. (2011). Surface wind direction variability. *Journal of Applied Meteorology and Climatology, 50*(1), 144-152.

Myers, K., (2007). *Environmentally conscious alternative energy production*. Hoboken: John Wiley & Sons, Inc.

Nobel Environmental Power (2012). The wind energy industry frequently asked questions. Retrieved from http:// www.noblepower.com/faqs/wind-energy-industry1.html

Noppel, H., & Fiedler, F. (2002). Mesoscale heat transport over complex terrain by slope winds – A conceptual model and numerical simulations. *Boundary-Layer Meteorology, 104*(1), 73-97.

Olsen, A., Wanninkhof, R., Trinanes, J. A., & Johannessen, T., (2005). The effect of wind speed products and wind speed-gas exchanges relationships on inter-annual variability of the air-sea CO2gas transfer velocity. *Tellus B*, 57(2), 95-106.

Ohsawa, T., Hashimoto, A., Shimada, S., Yoshino, J., De Paus, T., Heinemann, D., Lange, B. (2007). Evaluation of Offshore Wind Simulations with MM5 in the Japanese and Danish Coastal Waters. *European Wind Energy Conference & Exhibition EWEC, Milan, Italy, July 5-7, 2007.*

Parkinson, K. (2001). *Environmental Consequences of Offshore Wind Power Generation.* Retrieved from University of Hull: Institute of Estuarine and Coastal Studies

Pielke, R. A., Cotton, W. R., Walko, R. L., & et al. (1992). A comprehensive meteorological modeling system - RAMS. *Meteorological and Atmosphere Physics*, 49(1-4), 69-91.

Pielke, R. A., (2002). *Mesoscale meteorological modeling* (2nd ed.). San Diego: Academic Press.

Pichugina, Y., Banta, R. Brewer, A. Hardesty, M., & Sandberg, S., 2011, March 17). Offshore measurements of wind flow characteristics aloft for wind energy using shipborne high resolution doppler LIDAR [PDF document]. Retrieved from http://www.esrl.noaa.gov/research/events/seas/Mar2011/SEAS_March2011_Pichugina.pdf

Poynting, J. H., & Thomson, J. J. (1906). *A textbook of physics: Heat* (2nd ed.). London: Charles Griffin & Company Ltd.

Roney, J. M. (2010, March 14). Eco-economy indicators. *Earth Policy Institute*. Retrieved from http://www.earth-policy.org/indicators/C49/wind_power_2012

Shimada, S., & Ohsawa, T. (2011). Accuracy and characteristics of offshore wind speeds simulated by WRF. *SOLA, 7*, 21-24.

Skamarock, W. C. (2004). Evaluating mesoscale NWP models using kinetic energy spectra. *Monthly Weather Review, 132*(12), 3019-3032.

Soren, K., Awerbuch S., & Monthorst, P. E. (2009). The economics of wind energy. European Wind Engery Association. Retrieved from http://www.ewea.org/fileadmin/ewea_documents/documents/00_POLICY_document/Economics_of_Wind_Energy__March_2009_.pdf

Sørensen, B. (2008). A new method for estimating off-shore wind potentials. *International Journal of Green Energy, 5*(3), 139-147.

Sumner, J., Watters, C. S., & Masson, C. (2010). CFD in wind energy: The virtual, multiscale wind tunnel. *Energies, 3*(5), 989-1013.

Uppala, S. M., KÅllberg, P. W., Simmons, A. J., Andrae, U., Bechtold, V. D. C., Fiorino, M., ... (2005). The ERA-40 re-analysis. *Quarterly Journal of the Royal Meteorological Society, 131*(612), 2961-3012.

Vincent, C. L., Draxl, C., & Nielsen J. R. (2010, March 30). Mesoscale meteorological models [PDF document]. Retrieved from http:// www.windpower.org/download/559/1_mesoscale_modelling_safety.pdf

Xue, M., Droegemeier, K. K., & Wong, V. (2000). The advanced regional prediction system (ARPS) – A multi-scale nonhydrostatic atmospheric simulation and prediction model. part I: Model dynamics and verification. *eteorology and Atmospheric Physics, 75*(3), 161-193.

Wind energy. (n.d.). University of Strathclyde Engineering, Energy Systems Research Unit - ESRU. Retrieved from http://www.esru.strath.ac.uk/EandE/Web_sites/01-02/RE_info/wind.htm

WWEA (2009). World wind energy report 2009. Retrieved from http:// www.wwindea.org/home/images/stories/worldwindenergyreport2009_s.pdf

APPENDIX A

ADDITIONAL FIGURES

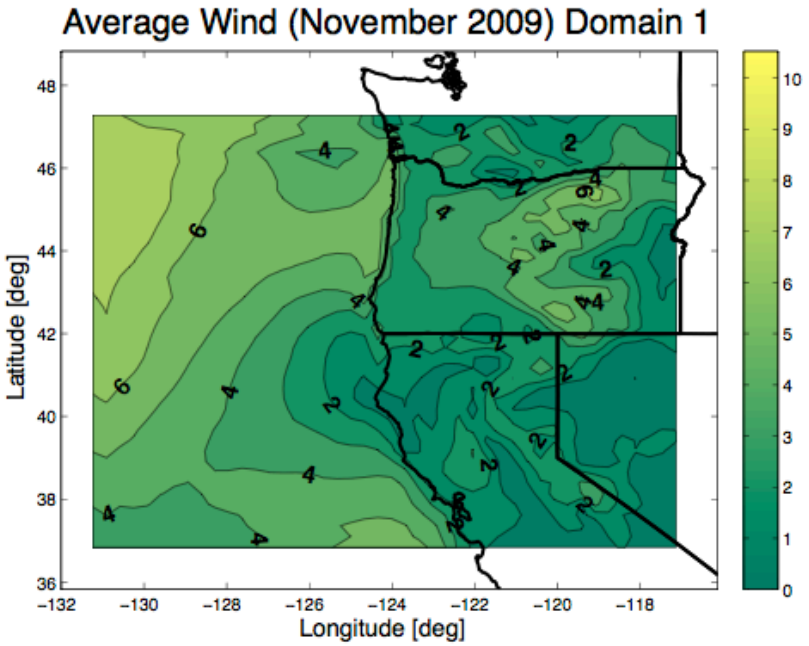

Figure A-1: Domain 1, Nov 2009, wind speed

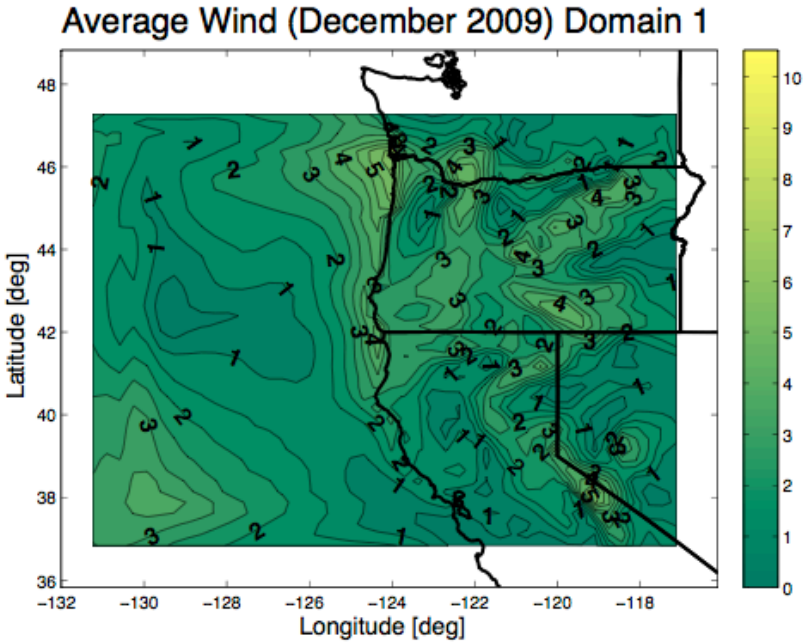

Figure A-2: Domain 1, Dec 2009, wind speed

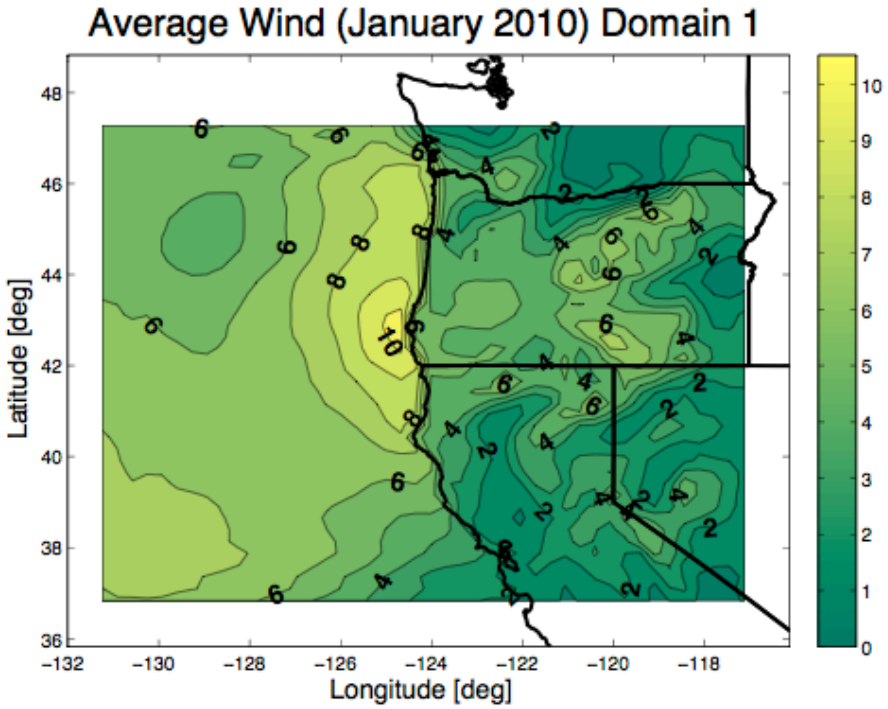

Figure A-3: Domain 1, Jan 2010, wind speed

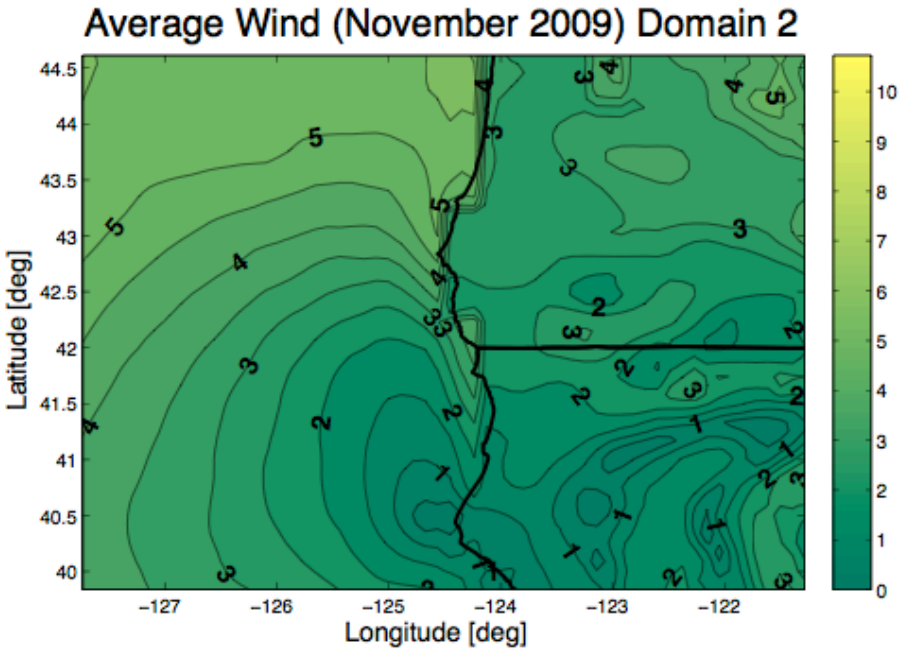

Figure A-4: Domain 2, Nov 2009, wind speed

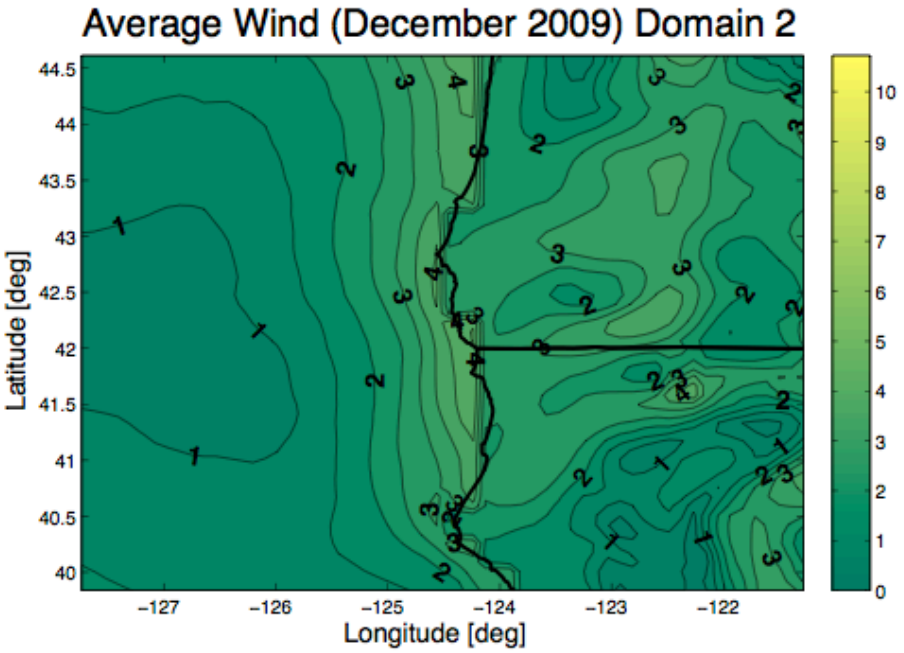

Figure A-5: Domain 2, Dec 2009, wind speed

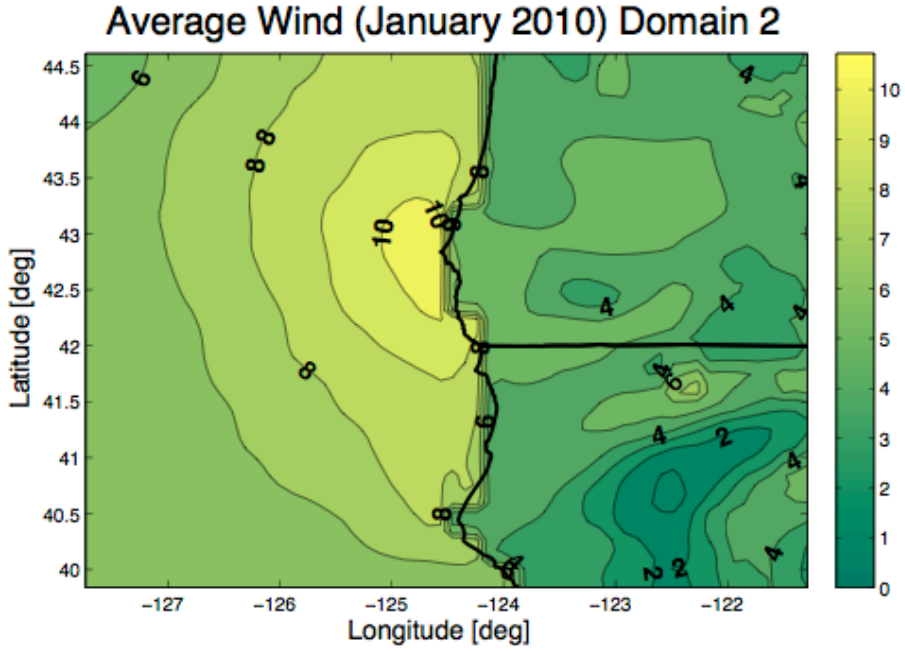

Figure A-6: Domain 2, Jan 2010, wind speed

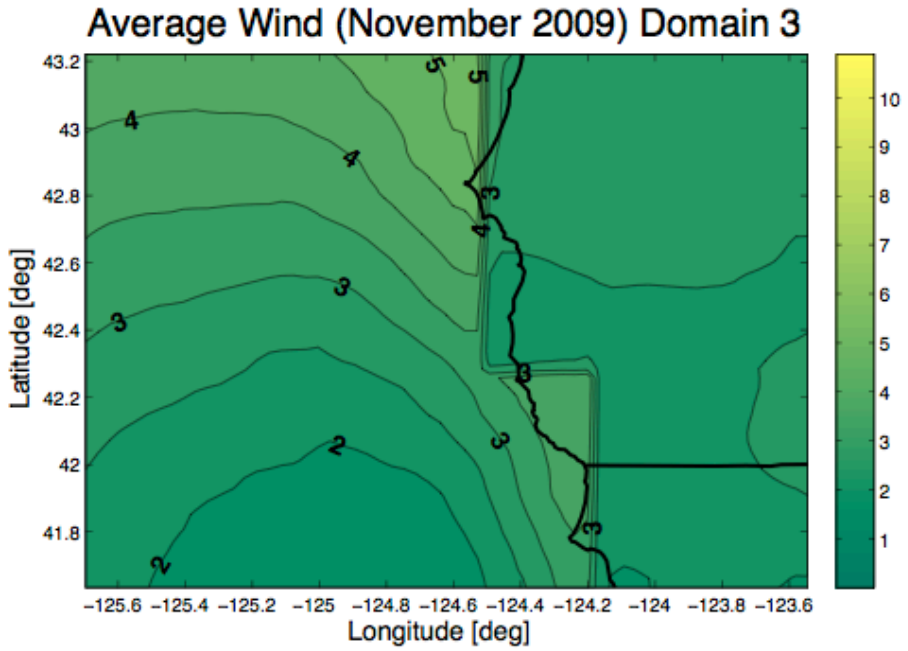

Figure A-7: Domain 3, Nov 2009, wind speed

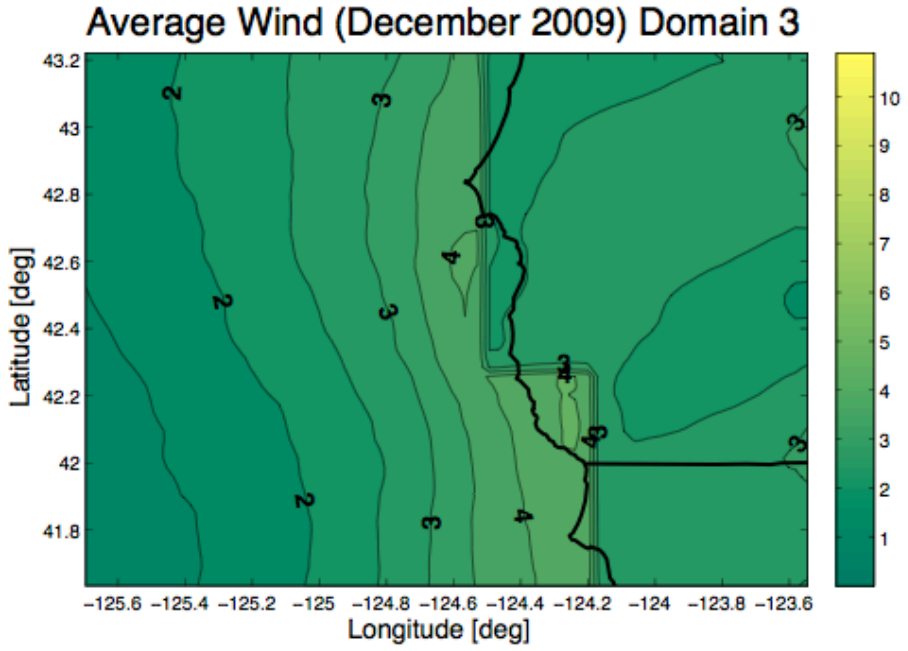

Figure A-8: Domain 3, Dec 2009, wind speed

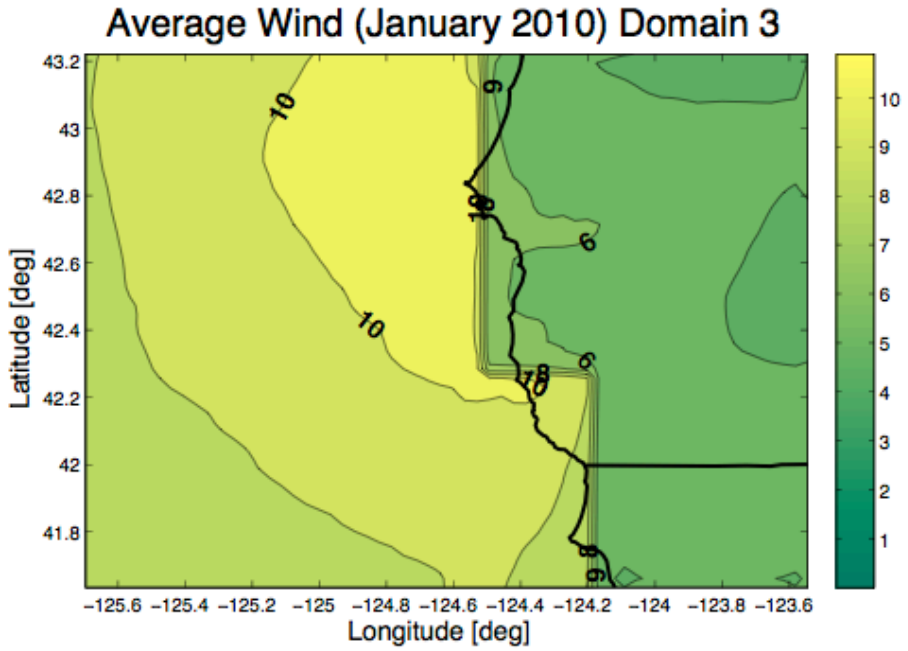

Figure A-9: Domain 3, Jan 2010, wind speed

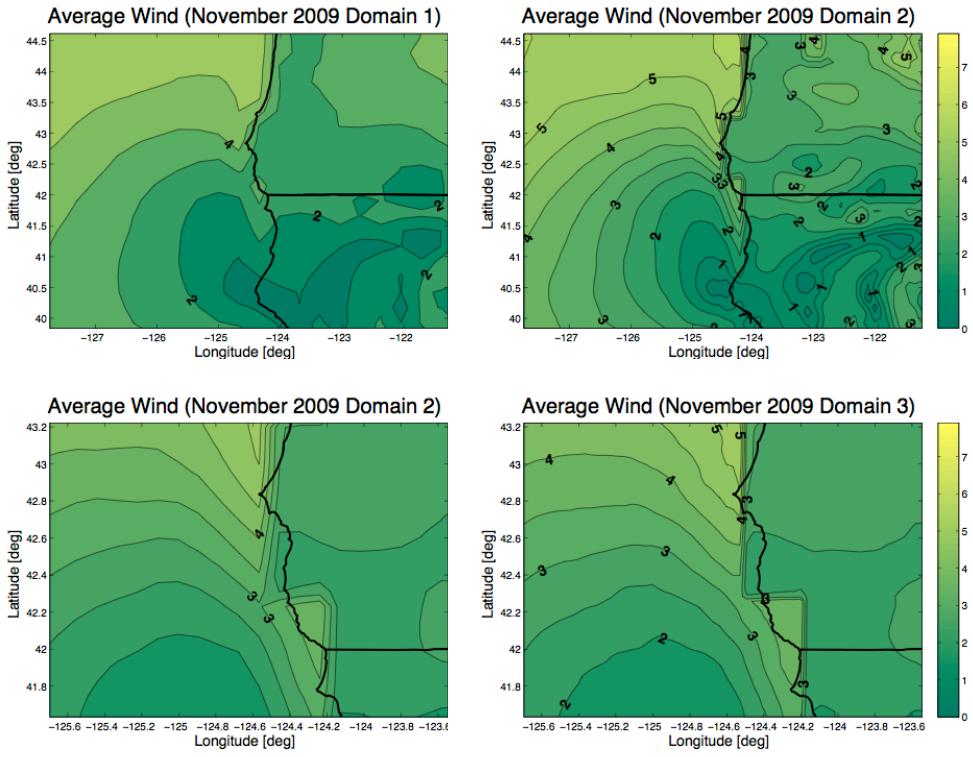

Figure A-10: Nov 2009, wind speed comparison

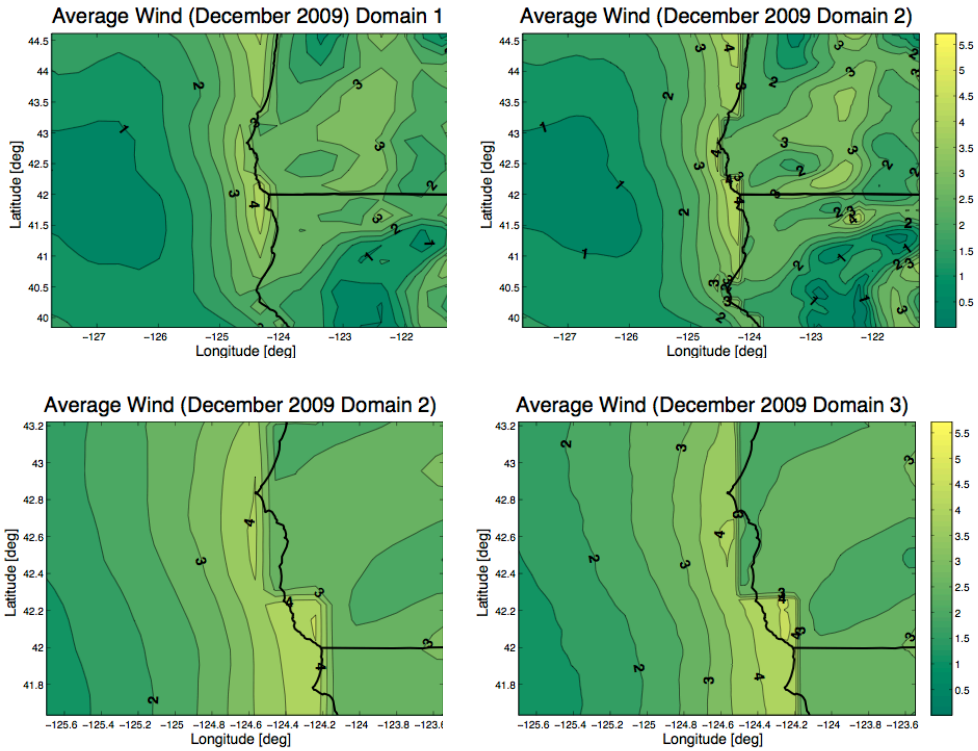

Figure A-11: Dec 2009, wind speed comparison

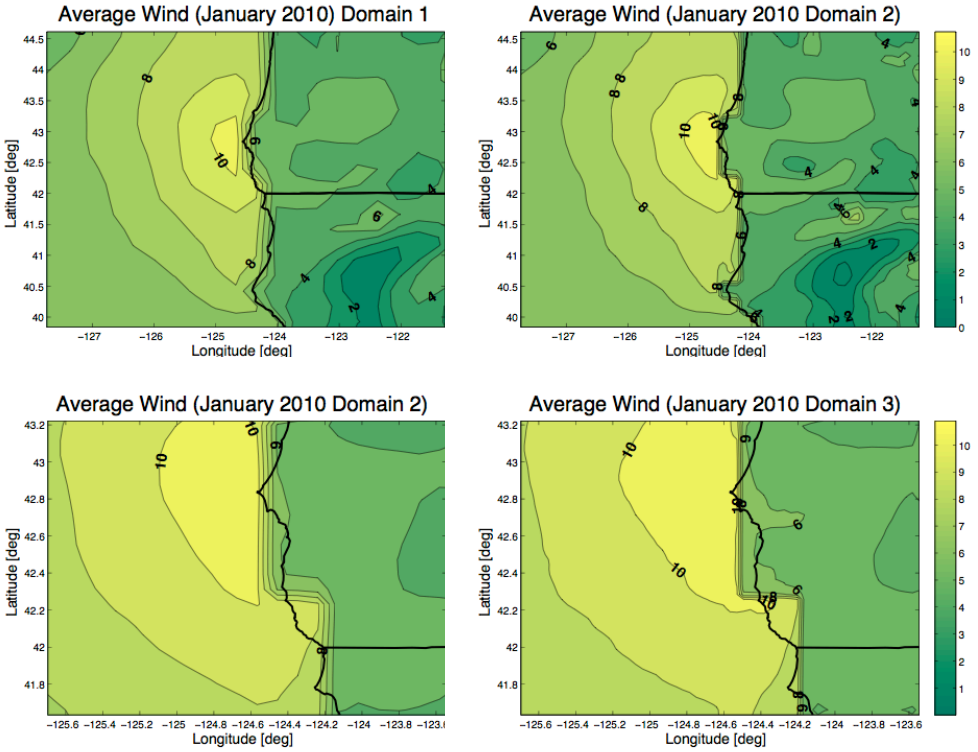

Figure A-12: Jan 2010, wind speed comparison

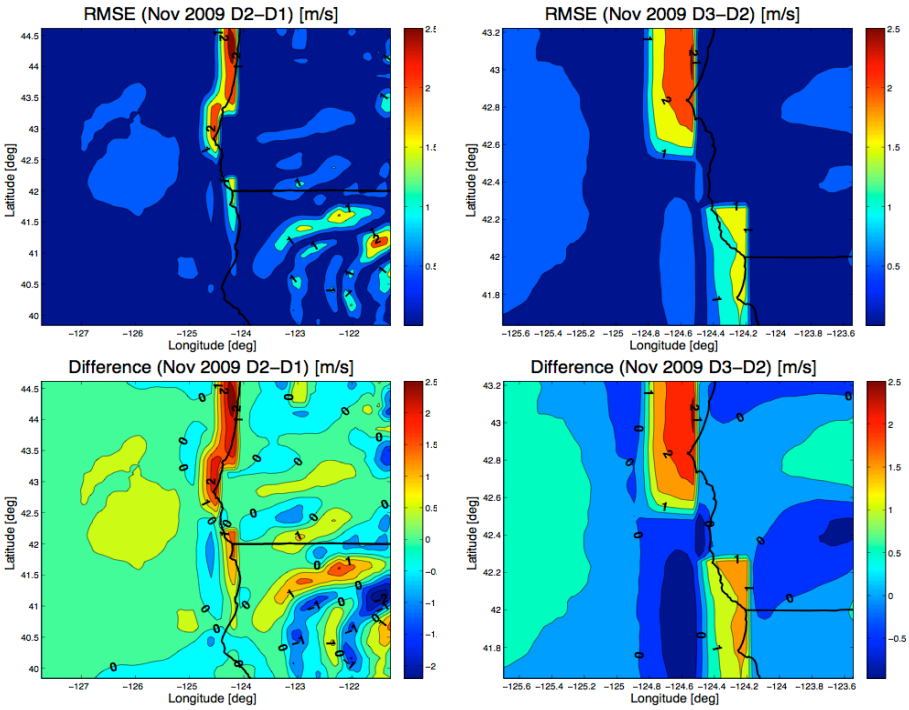

Figure A-13: Nov 2009, wind speed RMSE & bias

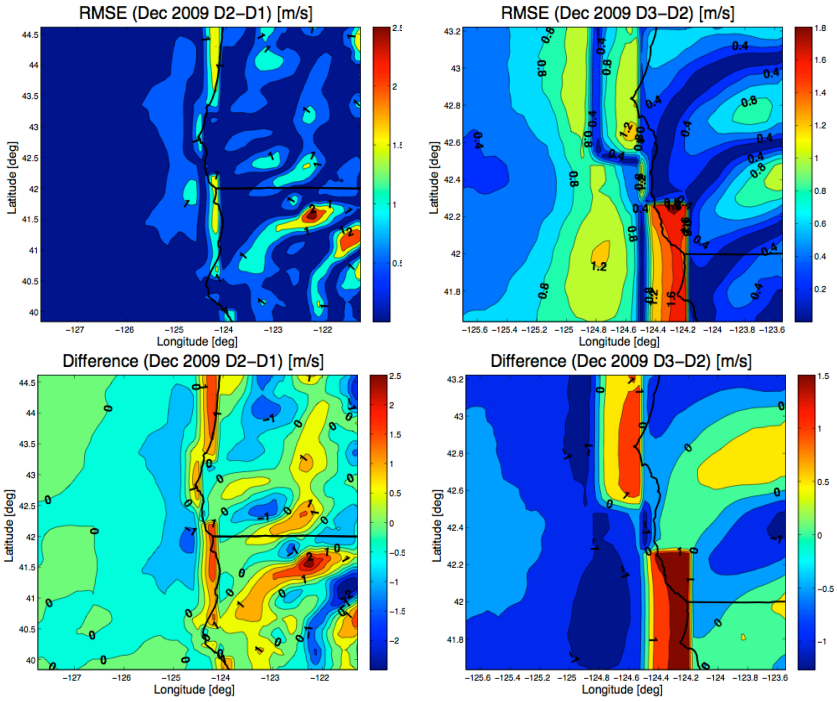

Figure A-14: Dec 2009, wind speed RMSE & bias

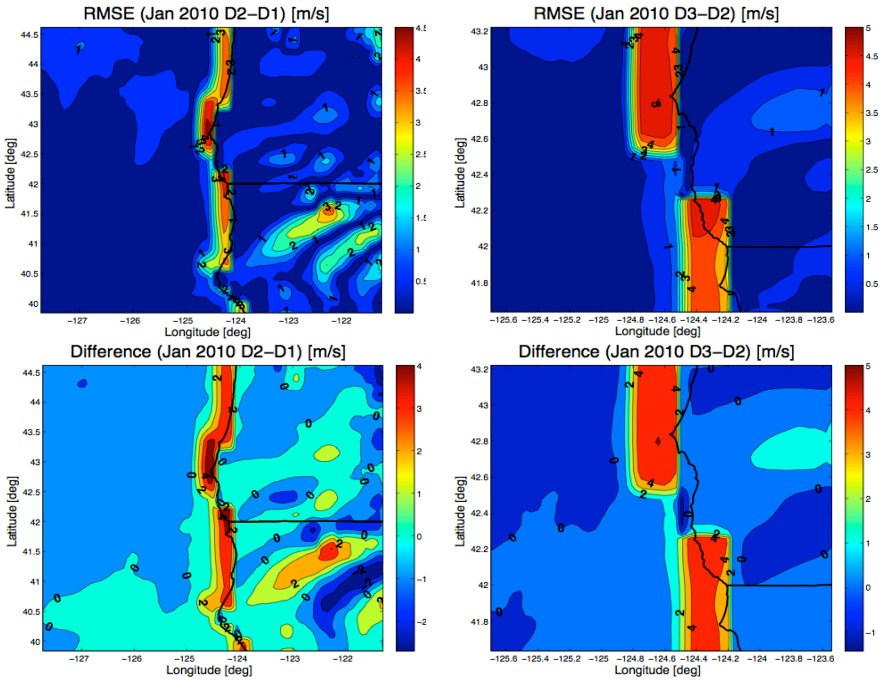

Figure A-15: Jan 2010, wind speed RMSE & bias

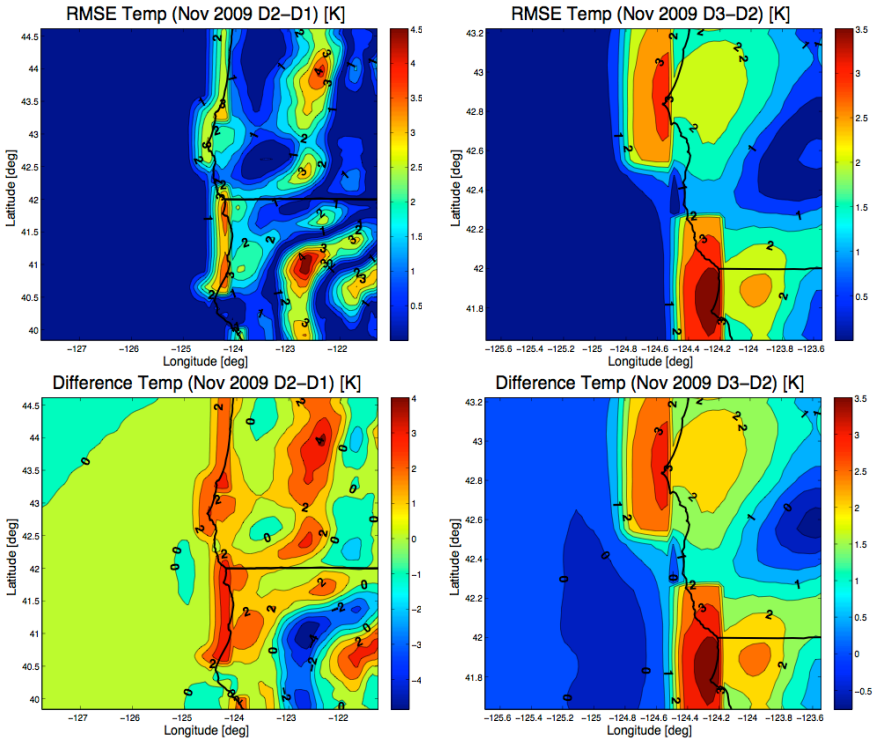

Figure A-16: Nov 2009, temperature RMSE & bias

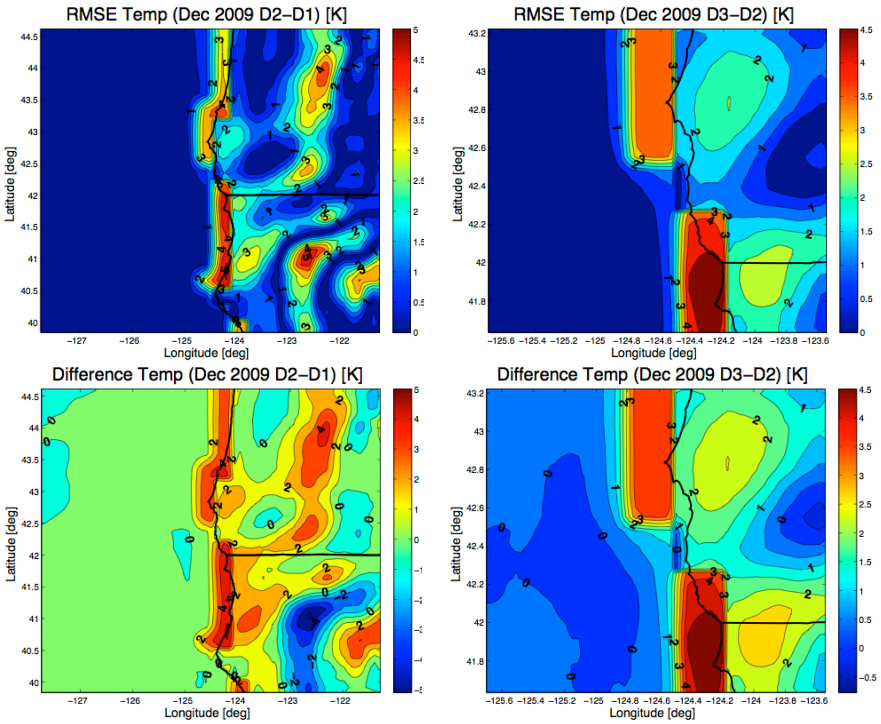

Figure A-17: Dec 2009, temperature RMSE & bias

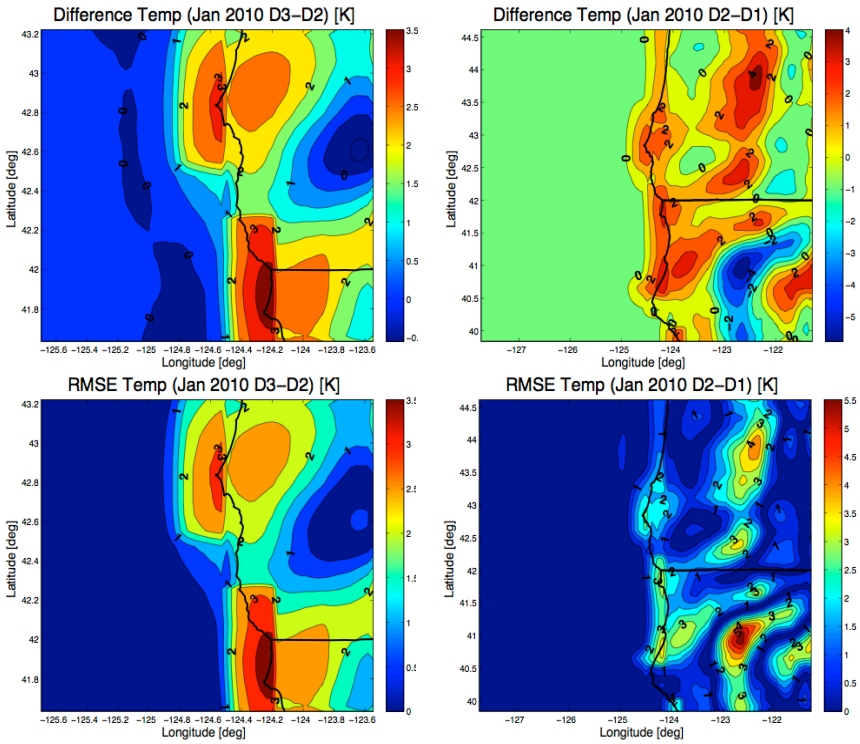

Figure A-18: Jan 2010, temperature RMSE & bias

APPENDIX B

ADDITIONAL TABLES

Offshore Domain					
Time & Domain		**RMSE**	**STD [m/s]**	$D_{i+1} - D_i$	**Bias [%]**
Nov 2009	D1	0.3637	0.6424	D2 - D1	316.91%
	D2	1.5163	0.6429	D3 - D2	14.15%
	D3	1.7308	0.8670	D3 - D1	375.89%
Dec 2009	D1	0.3374	0.4995	D2 - D1	225.55%
	D2	1.0984	0.5020	D3 - D2	12.35%
	D3	1.2341	0.3942	D3 - D1	265.77%
Jan 2010	D1	0.7798	1.0253	D2 - D1	432.01%
	D2	4.1486	1.2191	D3 - D2	12.39%
	D3	4.6627	2.4135	D3 - D1	497.94%
	Ave D1	0.4936	0.7224	Ave D2 - D1	324.82%
	Ave D2	2.2544	0.7880	Ave D3 - D2	12.96%
	Ave D3	2.5425	1.2249	Ave D3 - D1	379.86%

Table B-1: Offshore domain RMSE & bias statistics

Offshore Domain (WS)		
Time & Domain		**Corr. Coef.**
Nov 2009	D1	0.7924
	D2	0.5793
	D3	0.7557
Dec 2009	D1	0.0345
	D2	-0.0081
	D3	-0.4254
Jan 2010	D1	0.6457
	D2	0.4214
	D3	0.4999
	Ave D1	0.4909
	Ave D2	0.3309
	Ave D3	0.2767

Table B-2: Offshore domain wind correlation

BIOGRAPHICAL SKETCH

Having grown up the son of two former military members, work ethic in the Bouey household was never in short supply. Michael Bouey graduated from Moon Valley High School, Phoenix, Arizona, in 2000 and immediately left for the United States Army. After completing basic training, he was stationed at the NATO headquarters, SHAPE (Supreme Headquarters of Allied Powers Europe), Belgium. This duty station was followed by a combat tour at Abu Ghraib Prison, Iraq, January 2004. After completing his military service, Michael embarked on educational pursuits. Michael's academic achievements include the All-USA Today Academic Team Merit full-ride scholarship to Arizona State University (ASU). While attending ASU Michael participated in the Fulton Undergraduate Research Initiative, served as the Fulton Schools of Engineering Student Council President, graduated from Barrett, The Honors College, and graduated Magna Cum-Laude with a Bachelor's of Science in Mechanical Engineering. His graduate program focused on fluid mechanics and computational fluid dynamics. Michael's education has culminated with this thesis, "The Impact of Grid Resolution on Atmospheric Model Simulation of Offshore Wind Speed."